Geology and Geochemistry of Gold Deposits of the Big Canyon Area, El Dorado County, California
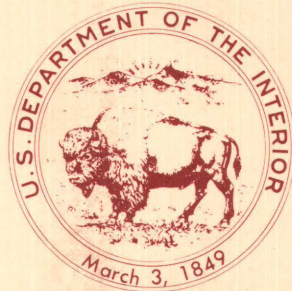
U.S. GEOLOGICAL SURVEY BULLETIN 1854

U.S. DEPARTMENT OF THE INTERIOR

March 3, 1849

AVAILABILITY OF BOOKS AND MAPS OF THE U.S. GEOLOGICAL SURVEY

Instructions on ordering publications of the U.S. Geological Survey, along with prices of the last offerings, are given in the current-year issues of the monthly catalog "New Publications of the U.S. Geological Survey." Prices of available U.S. Geological Survey publications released prior to the current year are listed in the most recent annual "Price and Availability List." Publications that are listed in various U.S. Geological Survey catalogs (see back inside cover) but not listed in the most recent annual "Price and Availability List" are no longer available.

Prices of reports released to the open files are given in the listing "U.S. Geological Survey Open-File Reports," updated monthly, which is for sale in microfiche from the U.S. Geological Survey, Books and Open-File Reports Section, Federal Center, Box 25425, Denver, CO 80225. Reports released through the NTIS may be obtained by writing to the National Technical Information Service, U.S. Department of Commerce, Springfield, VA 22161; please include NTIS report number with inquiry.

Order U.S. Geological Survey publications by mail or over the counter from the offices given below.

BY MAIL

Books

Professional Papers, Bulletins, Water-Supply Papers, Techniques of Water-Resources Investigations, Circulars, publications of general interest (such as leaflets, pamphlets, booklets), single copies of Earthquakes & Volcanoes, Preliminary Determination of Epicenters, and some miscellaneous reports, including some of the foregoing series that have gone out of print at the Superintendent of Documents, are obtainable by mail from

U.S. Geological Survey, Books and Open-File Reports
Federal Center, Box 25425
Denver, CO 80225

Subscriptions to periodicals (Earthquakes & Volcanoes and Preliminary Determination of Epicenters) can be obtained ONLY from the

Superintendent of Documents
Government Printing Office
Washington, D.C. 20402

(Check or money order must be payable to Superintendent of Documents.)

Maps

For maps, address mail orders to

U.S. Geological Survey, Map Distribution
Federal Center, Box 25286
Denver, CO 80225

Residents of Alaska may order maps from

Alaska Distribution Section, U.S. Geological Survey,
New Federal Building - Box 12
101 Twelfth Ave., Fairbanks, AK 99701

OVER THE COUNTER

Books

Books of the U.S. Geological Survey are available over the counter at the following Geological Survey Public Inquiries Offices, all of which are authorized agents of the Superintendent of Documents:

- **WASHINGTON, D.C.**--Main Interior Bldg., 2600 corridor, 18th and C Sts., NW.
- **DENVER, Colorado**--Federal Bldg., Rm. 169, 1961 Stout St.
- **LOS ANGELES, California**--Federal Bldg., Rm. 7638, 300 N. Los Angeles St.
- **MENLO PARK, California**--Bldg. 3 (Stop 533), Rm. 3128, 345 Middlefield Rd.
- **RESTON, Virginia**--503 National Center, Rm. 1C402, 12201 Sunrise Valley Dr.
- **SALT LAKE CITY, Utah**--Federal Bldg., Rm. 8105, 125 South State St.
- **SAN FRANCISCO, California**--Customhouse, Rm. 504, 555 Battery St.
- **SPOKANE, Washington**--U.S. Courthouse, Rm. 678, West 920 Riverside Ave..
- **ANCHORAGE, Alaska**--Rm. 101, 4230 University Dr.
- **ANCHORAGE, Alaska**--Federal Bldg, Rm. E-146, 701 C St.

Maps

Maps may be purchased over the counter at the U.S. Geological Survey offices where books are sold (all addresses in above list) and at the following Geological Survey offices:

- **ROLLA, Missouri**--1400 Independence Rd.
- **DENVER, Colorado**--Map Distribution, Bldg. 810, Federal Center
- **FAIRBANKS, Alaska**--New Federal Bldg., 101 Twelfth Ave.

Geology and Geochemistry of Gold Deposits of the Big Canyon Area, El Dorado County, California

By J. THOMAS NASH

Description of geology and geochemistry of two types of lode gold deposits in metamorphic rocks and their similarities to nearby Mother Lode deposits

U.S. GEOLOGICAL SURVEY BULLETIN 1854

CONTENTS

FIGURES

TABLES

METRIC CONVERSION FACTORS

For readers who wish to convert measurements from the metric system of units to U.S. customary units, the conversion factors are listed below.

Metric unit	Multiply by	To obtain U.S. customary unit
micrometer (μm)	3.937×10^{-5}	inch
millimeter (mm)	3.937×10^{-2}	inch
centimeter (cm)	3.937×10^{-1}	inch
meter (m)	3.281	foot
kilometer (km)	6.214×10^{-1}	mile
degree Celsius (°C)	[degree Fahrenheit (°F)–32]/1.8	

Geology and Geochemistry of Gold Deposits of the Big Canyon Area, El Dorado County, California

J. Thomas Nash

Abstract

Gold deposits in metamorphosed Phanerozoic rocks of the Big Canyon area, El Dorado County, California, yielded more than $3 million worth of ore prior to 1940. The deposits are in metamorphosed mafic extrusive and intrusive rocks, pyritic chert, and lean banded iron-formation of the Bear Mountains ophiolitic melange, just west of a major fault zone in Big Canyon that separates them from Upper Jurassic volcanic and clastic rocks that host the Mother Lode. The melange is a mostly chaotic assemblage of mafic volcanic rocks and mafic and ultramafic intrusive rocks, as well as metachert and banded iron-formation, of which the latter may have lateral continuity. These rocks were metamorphosed to greenschist grade in the Nevadan orogeny. Faults that influence the distribution of gold splay westward from the major fault, commonly with flat dips, and cut Upper Jurassic rocks.

Gold deposits occur in two settings: (1) faulted and brecciated Paleozoic basaltic metatuff and metadiorite that have pyrite-carbonate-albite alteration and veining, as at the Big Canyon mine; and (2) weakly fractured, seemingly stratiform deposits in Paleozoic pyritic metachert and adjacent pyrite-carbonate-albite-altered balsaltic metatuff, as at the Vandalia mine. The Big Canyon mine was one of the largest lode gold mines in El Dorado County. Substantial marginal reserves of gold are indicated by drilling and workings at the Big Canyon mine and Live Oak prospect, and additional large inferred resources may occur in similar settings that display pyrite-carbonate-albite alteration along faults subsidiary to the Big Canyon fault. The Vandalia deposit may be unique in the Sierra Nevada foothills because comparable thicknesses of pyritic metachert have not been recognized elsewhere.

The Big Canyon-type deposits contain multiple zones as much as 30 meters thick that are veined and flooded by pyrite-carbonate-albite, most of which contains more than 1 gram per ton Au. These zones are enriched in Na, Ca, Mn, P, S, and CO_2, as well as As, Sb, Se, Te, and rare-earth elements, but lack notable enrichment in Ag, Cu, Pb, or Zn. Gold-rich pyritic metachert at the Vandalia mine also is enriched in the same suite of major and minor elements found in the Big Canyon-type deposits; minor fractures in metachert appear to have allowed ingress of fluids that redistributed pyrite and caused carbonate and albite to form in thin bands along bedding. The gold in the Big Canyon-type deposits is clearly related to structures that cut Upper Jurassic rocks, and the alteration cuts or overprints the prograde greenschist-facies (albite-epidote-actinolite) metamorphism. The pyritic metachert and associated lean banded iron-formation at the Vandalia mine probably originated as a volcanogenic exhalite; it could have contained gold as an original component, but more likely the gold was introduced along with other metals at the same time that the Big Canyon-type deposits formed.

Gold deposits of both structural types in Big Canyon are interpreted to be of the same age and formed by similar processes; differences in form relate to physical properties of host rocks, behavior of the host rocks in postmetamorphic deformation, and different reactivity of the host rocks to hydrothermal fluids. In both settings, reactions of sulfur with iron silicate, carbonate, and oxide minerals seem to be a key to the deposition of gold. These sulfidation reactions may be indirect indicators of gold-depositing reactions or could be directly involved. The similarity of structural controls, alteration minerals, and geochemical signatures suggests that the Big Canyon deposits are similar to gold deposits of the Mother Lode and some deposits in Archean greenstone belts. By analogy to those well-studied world-class deposits, and from evidence at Big Canyon, the deposits are believed to have formed from alkaline, CO_2-rich fluids of moderate temperature (300–400 °C?) and pressure (1–2 kilobars?) of metamorphic origin. If the analogy to the Mother Lode deposits is apt, large volumes of mafic rocks in the melange zone along its bounding suture should be favorable for the development of gold deposits.

INTRODUCTION

The western foothills of the Sierra Nevada, particularly the Mother Lode zone, have been important

producers of gold and other metals since the 1850's and are favorable for the occurrence of additional deposits and extensions of known deposits. The Big Canyon area (fig. 1), about 16 km southwest of Placerville and 7 km west of the Mother Lode belt, contains several gold deposits with substantial past production and indications of additional resources. This geochemical research was undertaken to contribute to the understanding of gold deposits in the area west of the famous Mother Lode belt and to determine possible similarities to the Mother Lode. Also, deposits of the two structural types in the Big Canyon area have similarities to world-class gold deposits in Archean greenstone belts elsewhere in the world, although those in El Dorado County are of Phanerozoic age and are not as highly metamorphosed or deformed. The gold deposits in metachert at the Vandalia mine resemble those recently discovered at Hemlo, Ontario, and seem to be one of the rare examples in the United States that might provide an analog for geochemical processes that may have formed the giant deposits at Hemlo. This report does not provide a complete explanation for the origin of these types of deposits, but the petrologic and geochemical descriptions, and possibly the interpretations, should be helpful to workers concerned with evaluation of gold deposits in metamorphic rocks.

In 1983, Gold Fields Mining Corp.[1] examined the Big Canyon area and recognized a potential for both high-grade vein deposits and bulk-minable near-surface deposits. Surface exploration and drilling in the period 1983–1985 intersected many zones with gold grades in the range of 3–7 g/t (grams per ton, the same as parts per million), but the drilling was not sufficiently close spaced to define a mining reserve (R. Ridler, Gold Fields Mining Corp., oral commun., 1985). Environmental opposition to openpit mining was a factor that caused Gold Fields Mining Corp. to stop its exploration program in 1985 after drilling about 40 holes, most of which intercepted zones that contain more than 1 g/t Au. In 1986, an El Dorado County company acquired the Big Canyon and Vandalia properties and continued feasibility studies.

METHODS OF STUDY

Geologic studies by Gold Fields Mining Corp. (Osterberg and others, 1984), and about 12,000 m of drill core, provided an excellent starting point for geochemical studies of host rocks and ores, which commenced in May 1985. This study is chiefly based on observations made on

---

[1]The use of industry or firm names in this report is for location purposes only and does not impute responsibility for any present or potential effects on the natural resources.

drill core and on about 120 samples collected while logging core. A magnetic susceptibility meter was used to test drill core for the presence of magnetic minerals such as pyrrhotite and magnetite. Brief studies were made of surface geology, but it was felt that the rocks were too weathered for petrologic and chemical studies of primary features. Samples selected for chemical study were sawn from drill core; samples of about a quarter of the core were 0.3 m in length and weighed about 1 kg. A slice of the sample was retained for petrographic study. A total of 82 samples were submitted for chemical analyses. The samples are described in Appendix I. Thin sections, most with polished surfaces, were prepared from 98 samples. Chemists of the U.S. Geological Survey utilized X-ray fluorescence (XRF), induction-coupled plasma spectrometry (ICP), and wet chemical methods for the analysis of more than 40 major, minor, and trace elements. The methods and results of analyses and limits of detection are explained in Appendix II. Transmitted- and reflected-light microscopic study of the thin sections utilized high-power oil-immersion objectives to identify fine mineral grains and their paragenetic relations to gold.

ACKNOWLEDGMENTS

MINING HISTORY

The Big Canyon (or Oro Fino) and Vandalia deposits (fig. 2) were discovered in the early 1880's, and underground workings were soon developed (Logan, 1938; Clark and Carlson, 1956). The Big Canyon mine
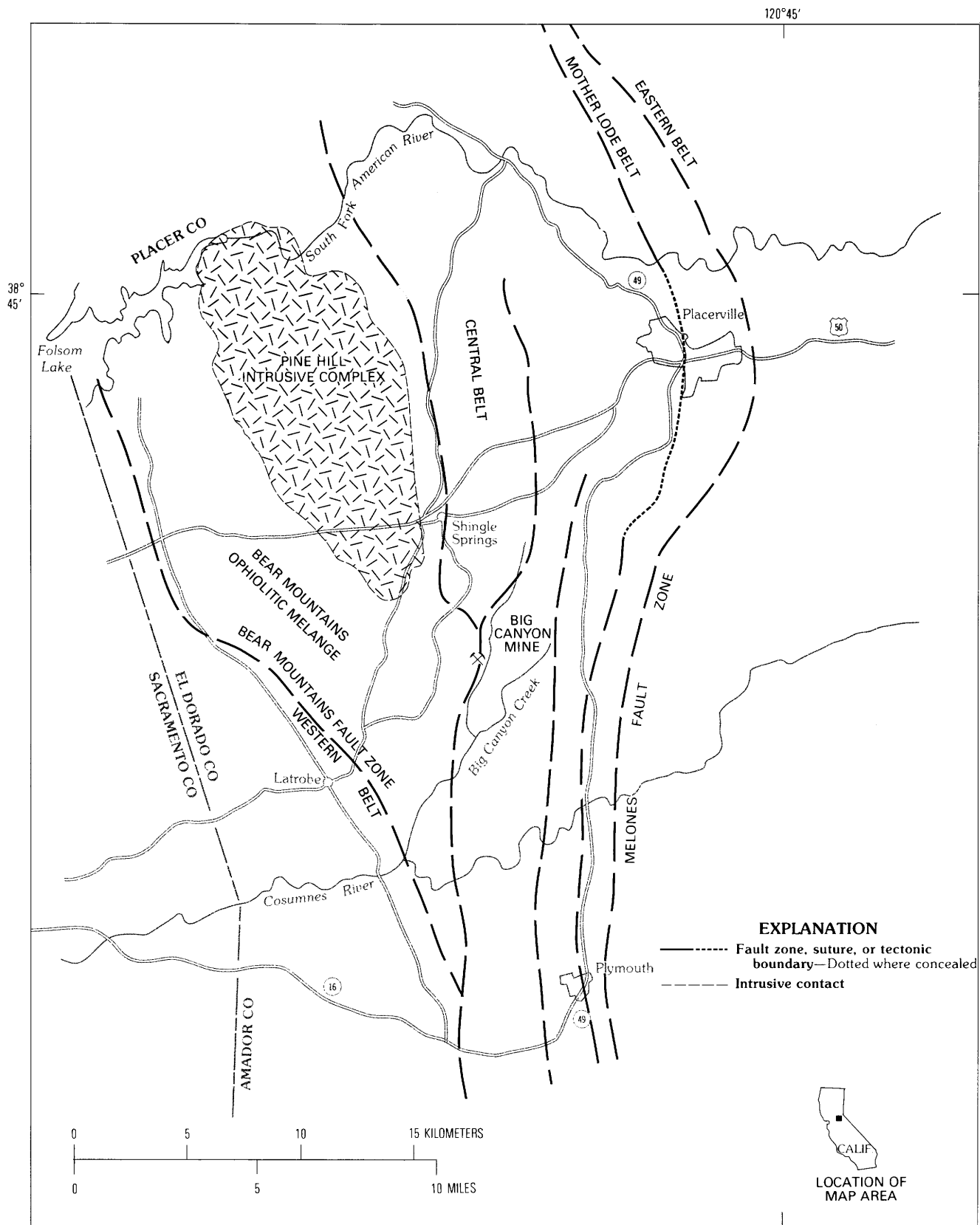
Figure 1. Tectonic belts in the Sierra Nevada foothills and location of the Big Canyon mining area. Tectonic belts are from Clark (1976), Duffield and Sharp (1975), Saleeby (1982), Loyd and others (1983), and Wagner and others (1981).

was one of the most productive lode gold mines in El Dorado County; it produced more than $3 million in gold during 1893–1901 and 1934–1940. The Vandalia mine, which had substantial underground workings, produced only small amounts of gold in 1888, 1900, and 1926–1928 (Logan, 1938). The mines, which have not operated since 1940, are not accessible, but useful information is reported by Logan (1938) and Clark and Carlson (1956). The Big Canyon mine had a 20-stamp mill prior to 1888 and was particularly productive between 1893 and 1901, during which time 180,000 tons of ore yielded $720,000 (Logan, 1938, p. 220). During that period mining reached the 500-ft level. The flatly dipping ore shoot had a maximum length of 450 ft (137 m) and a thickness of about 60 ft (18 m). From 1934 to 1940 the workings were extended deeper and along strike; the average dip of veins was about 35° E. and the strike was S. 25° W. (Logan, 1938). The ores from high levels were successfully treated by amalgamation, but that was not effective on the deeper pyritic ores which were treated by flotation. On February 26, 1937, water from Big Canyon Creek flooded the mine. Later in 1937 an openpit was developed to reach ore below the 100-ft level. The Big Canyon mine was forced to close in 1940 by the War Production Board Limitation Order.

Logan (1938, p. 220–221) described the wall rocks in the Big Canyon deposit as altered meta-andesite breccia with a

> dike of serpentine between it and the Calaveras (Carboniferous) hanging-wall rocks. On the west it merges with amphibolite schist... The good ore has been found to consist of about equal parts of albite, ankerite, and quartz, of which albite appears to be necessary, or at least highly favorable, for gold deposition. Rock of very similar appearance superficially, and provisionally termed quartzite, but lacking the albite, does not make good ore. J.M. Basham, superintendent, reports three periods of sulphide mineralization. The first is of arsenopyrite, the second of barren pyrite, and the third of auriferous pyrite.

The Vandalia mine produced about 14 tons per day in 1888, but there are no records of much production in later years despite several attempts (Logan, 1938, p. 254). The ore mined in 1888 was described by miners as "partly honeycombed quartz and partly very sulphuretted rock" (Logan, 1938, p. 254). According to Logan (1938, p. 254)

> the geology in general is similar to that of numerous sulfide deposits in the county in which amphibolite schist and the rocks interbedded with it have been silicified and impregnated with pyrite which is more or less auriferous. The oxidized, upper parts of the bodies rich in sulfide yielded the ore of early days. Two ore shoots 20 ft (6 m) thick and 50 ft (15 m) and 100 ft (30 m) long, respectively, were reported. The lowest of the

old adits reached the fresh sulfide at the bottom of the oxidized zone, and this has evidently not yielded enough gold, so far as opened, to pay a profit.

Quoting observations made in 1900, Clark and Carlson (1956, p. 428) reported that dimensions for the Vandalia orebodies were somewhat larger and that ore commonly cuts the schistosity of enclosing wall rocks.

Although some of the terms and concepts of the early miners are not accepted today, their observations are still a pertinent framework for economic geology and geochemistry.

GEOLOGIC SETTING

The Big Canyon area is in the west-central foothills of the Sierra Nevada (fig. 1) in a structurally complex zone called the melange belt by Duffield and Sharp (1975) and renamed the Bear Mountains ophiolitic melange by Saleeby (1982); the simpler term, melange belt, will be used here. The Mother Lode belt with its productive gold deposits is about 7 km to the east (Loyd and others, 1983). The Mother Lode fault system, which is about 190 km in length (Knopf, 1929), coincides with or is near the Melones fault zone, a major north-trending suture. The Melones fault juxtaposes Paleozoic rocks intruded by Mesozoic granitic rocks of the Sierra Nevada batholith on the eastern side with Mesozoic metavolcanic and metasedimentary rocks on the western side. It was probably active in the Late Jurassic (Duffield and Sharp, 1975). Geochronologic studies of Mother Lode mineralization (Bohlke and Kistler, 1986) yield K/Ar ages of about 110–125 Ma, or about 30 m.y. after the peak of magmatism and metamorphism of the Nevadan orogeny. The Mother Lode belt is composed of Upper Jurassic clastic and volcanic rocks. The western limit of the Mother Lode belt of Jurassic rocks is a north-trending high-angle fault of regional extent; the segment in Big Canyon is here termed the Big Canyon fault zone for its importance in localizing gold deposits at the Big Canyon mine and other prospects to the south. The western boundary of the melange belt is the Bear Mountains fault zone (Clark, 1964; Duffield and Sharp, 1975) about 7 km to the west of the Big Canyon mine.

The melange belt has been described as a chaotic assemblage of highly faulted and sheared clastic, volcaniclastic, and mafic intrusive rocks and serpentinite (Duffield and Sharp, 1975). There are differences of opinion regarding the degree of tectonic disruption in the belt with many workers favoring multiple stages of dismemberment and tectonic emplacement of mixed blocks of diverse rock types during subduction and accretion (Saleeby, 1982; Landefeld and others, 1986; Earhart,
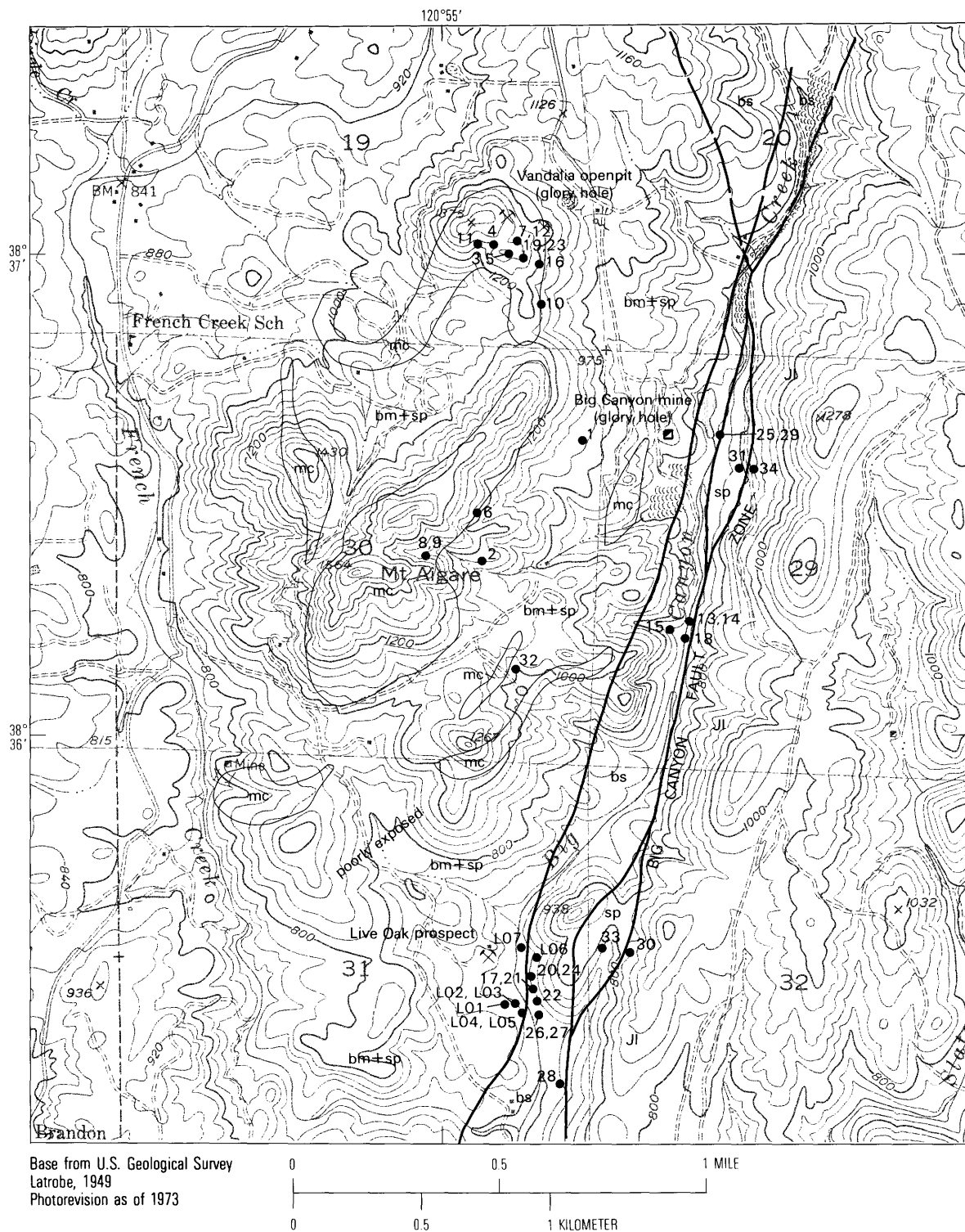
Figure 2. Generalized geology and location of drill holes, Big Canyon area. Geology is simplified from Osterberg (1984). Most of the area west of the Big Canyon fault has very poor outcrops and is underlain chiefly by Paleozoic basaltic metatuff and altered ultramafic rocks.

1988). However, regional mapping of distinctive lithologies by Gold Fields Mining Corp. personnel suggests some units that can be traced for as much as 25 km on strike are not totally chaotic (M. Osterberg, Gold Fields Mining Corp., written commun., 1987). Local areas are coherent and have conformable layering, which suggests they are kilometer-sized "clasts" in a megabreccia. One possible large "clast" (Earhart, 1988) is locally important at the Vandalia mine and Mt. Aigare (fig. 2) where a coherent unit of predominantly cherty rocks is exposed over an area about 3 km long by 0.5 km wide and is about 150 m thick according to drilling. An alternative interpretation is that the cherty sequence can be traced on strike and thus is not composed of exotic blocks (M. Osterberg, Gold Fields Mining Corp., written commun., 1987) rafted into place by submarine slides or accretionary tectonics. Mafic volcanic and intrusive rocks, which are most characteristic of the melange belt, have been interpreted as dismembered parts of an ophiolite sequence (Saleeby, 1982). The belt includes some of the oldest known rocks west of the Sierra Nevada batholith according to lead isotopic ages of 200–300 Ma (Saleeby, 1982). The Pine Hill intrusive complex (Springer, 1980) intruded and metamorphosed the Bear Mountains ophiolitic melange; this complex provides an important age reference of 162 Ma (Saleeby, 1982). The Big Canyon area is at the intersection of several major structures; the major questions about structure and stratigraphy of both the regional and local settings of the gold deposits remain unanswered.

GEOLOGY OF THE BIG CANYON AREA

The geology of the area (fig. 2) is more complex than shown on published regional maps. Recent mapping (Osterberg and others, 1984; R. Earhart, written commun., 1987) has clarified the structure, but ambiguities remain because of very poor outcrop in key areas. No stratigraphy can be established in Paleozoic rocks of the area, and tops of bedded units generally are not known. Metamorphism to greenschist facies obscures some lithologic features but is not so intense or variable as to cause problems in recognition of units or in the interpretation of protolith. At least five generalized lithologic units can be used in mapping and in logging of drill core. Layered pyroclastic rocks of basaltic composition are most abundant in and near the deposits; these are now epidote-amphibole-quartz-albite±calcite rocks with layered or schistose fabrics that I will term basaltic metatuff. Light-colored, finely laminated metasedimentary rocks are common on the ridge from Vandalia mine to Mt. Aigare; these are chiefly metachert with variable amounts of pyrite, hematite, and magnetite along bedded layers. In most places the metachert contains less than 5

percent iron minerals, but a few outcrops found by Earhart (1988) contain more than 15 percent hematite and magnetite, and those beds can be called banded iron-formation (BIF). Outside of the ore deposits mafic and ultramafic intrusive rocks are common; these rocks, which were peridotite and diorite, have been metamorphosed to serpentinite and amphibolite. Metamorphosed debris flows have been recognized by R. Earhart (written commun., 1986); they contain coarse fragments (about 10–50 cm in size) of basaltic rocks, chert, and exotic metamorphic rock fragments. Black slate and argillite occur in fault slices within the Big Canyon fault zone (fig. 2); the age of this unit is not known. The area east of the Big Canyon fault (fig. 2) is underlain by weakly metamorphosed volcanic rocks of the Jurassic Logtown Ridge Formation (Duffield and Sharp, 1975), which is chiefly basaltic tuff, breccia, and flows. The Big Canyon fault zone and many other faults in the area contain highly sheared serpentinite that may have been mechanically intruded as a ductile rock.

Most structures in the area must be inferred because they occur in areas of low relief with very poor outcrop. Drill-core information helps define the position of faults but is not good for defining attitudes or offset. Structures that juxtapose rock types, some of which control the distribution of gold, could be the sites of either major dislocations or possibly only small displacements.

GOLD DEPOSITS

Two structurally distinct types of gold deposits occur in the Big Canyon area. The Big Canyon type, best illustrated by the Big Canyon mine, is structurally controlled by numerous closely spaced fractures in the Big Canyon fault zone. Gold is consistently associated with zones of PCA (pyrite-carbonate-albite) alteration of mafic rocks and vein filling. Relations observable in the glory hole of the Big Canyon mine and in drill core indicate that the alteration zones and gold mineralization are in basaltic metatuff and metadiorite that are in fault contact with serpentinite, slate, and black argillite. The serpentinite and argillite, which are locally altered and chemically modified, contain only traces of gold; these rocks evidently were chemically or physically unfavorable for significant gold mineralization. Another area of PCA alteration in fractured mafic rocks occurs 2 km south of the Big Canyon mine at the Live Oak prospect (fig. 2) in an area that was drilled by Gold Fields Mining Corp. and found to contain many intercepts with more than 1 g/t Au. Excellent examples of PCA alteration and gold were recovered from drill core for this study.

The second type of deposit, known at the Vandalia mine, occurs in pyritic metachert and to a lesser extent in altered basaltic metatuff. These stratified rocks are

folded and faulted, and some pyrite occurs on fractures, but the gold-pyrite mineralization appears to be stratiform—although "beds" of ore have not been traced laterally in mine workings or drill holes, and the bedded nature of the minerals in hand specimen does not prove that they formed syngenetically with the enclosing sediment. Gold Fields Mining Corp. personnel interpreted the ore-bearing strata at Vandalia to have been originally a chemical sediment or exhalite. There is abundant evidence in support of the exhalite concept, but as will be discussed later, there also is substantial evidence for epigenetic metasomatism of the type that is well developed at the Big Canyon mine. The geometry and wall rocks of the Vandalia and Big Canyon types of gold deposits are clearly different, but new geochemical and petrographic data suggest that the two types of gold ores are geochemically similar and most likely formed at the same time.

Structure at the Big Canyon mine and Live Oak prospect is too complex to be illustrated here. A series of vertical and angle core holes were collared east of the gold deposits to test for mineralization in the Big Canyon fault zone and beneath the surface exposures. Most of the rock recovered in core from those holes is extremely fractured and sheared. Although the general distribution of units in Big Canyon suggests a high-angle fault (fig. 2), the structure is much more complex in detail and no logical cross sections can be drawn from information from holes that were drilled 100 m apart. The Big Canyon structure is a series of subparallel high-angle faults in a zone more than 100 m wide with branching low-angle faults that cut off blocks between the high-angle faults. My impression from drill core is a chaotic jumble of blocks, each about 10–20 m wide (E–W) and deep and of uncertain length (N–S), with abundant internal shear. Blocks of slate, argillite, and serpentinite are most common on the eastern side of the fault zone. The metasediments and serpentinite on the eastern side are only rarely cut by PCA alteration, and only a few assays show any detectable gold (more than 0.1 ppm). On the western edge of the fault zone blocks of relatively coherent mafic rocks are encountered, and in the mineralized areas the mafic rocks tend to be bleached from dark green to tan and highly altered to PCA from the fault contact westward. For 100–200 m westward the mafic rocks are cut by fractures with prominent tan alteration selvedges. One of the mineralized units at the Live Oak prospect is a brecciated metadiorite; the geometry of the intrusive contact is not known, but it is clear that the diorite was brecciated prior to alteration. I saw no metachert in drill holes from the Big Canyon-type deposits.

All gold mineralization in the Big Canyon and Live Oak deposits is associated with fracture filling and wall-rock alteration, which consists of tan carbonate and albite with 2–10 percent pyrite. Megascopically the pyrite, tan color, and hardness are obvious, as are late-stage light-colored carbonate veinlets that effervesce violently in dilute acid. However, the albite and noneffervescing carbonate (ankerite) replacement are not easily distinguished megascopically from silicic alteration. The association of gold and pyrite with albite and ankerite rather than with quartz is clearly seen in thin sections.

Structural style in the Vandalia gold deposit is much different from that of the Big Canyon-type deposits. The layered rocks are folded, probably twice, and fractured, but faults are not a major feature. Drilling density is not sufficient to document the likely continuity of pyritic layers at deposit scale, but outcrop features do suggest the continuity of some pyritic layers for hundreds of meters (Osterberg and others, 1984). There may be systematic facies variations in pyrite, hematite, and magnetite concentrations in the cherty sequence, as in iron formations elsewhere (James, 1954), but these have not been worked out. The major question about the structure and stratigraphy is the relationship of the cherty clastic rocks to basaltic metatuff. Earhart (1988) observed fault contacts between the two units in a few outcrops and inferred faults elsewhere as he reached the interpretation that the cherty sequence is a tectonic block in the melange. This may be correct, but some features revealed in drill core suggest other relations. All the drill holes in the northwestern part of the study area (fig. 2) intersect both metachert and basaltic metatuff, and in 11 drill cores more than one cherty unit is intercepted. Layers of metachert 1–2 m thick appear to be conformable with enclosing basaltic metatuff in five drill holes; these layers occur 50–100 m below the thick metachert sequence. Bedding attitudes are consistent in both metachert and basaltic metatuff over distances of 50–100 m in many holes, and although basaltic metatuff is broken adjacent to metachert in some cores, a major fault is not indicated or required—the fractures seen in core could as well be explained by folding. Petrographic and chemical analyses, which are described in the next section, reveal that the metachert and enclosing rocks have both been subjected to PCA alteration, and variable contents of Si, Al, and Ti suggest the possibility of mixing of tuffaceous and exhalative components during sedimentation. Also, both metachert and basaltic metatuff sequences are cut by similar diabase dikes, which are in turn subjected to PCA alteration. The metachert and basaltic metatuff were clearly contiguous prior to folding, metamorphism, and PCA alteration, regardless of how the units came together. The gold and pyrite could be syngenetic with the cherty exhalite and thus of Paleozoic age and much older than the Big Canyon-type gold mineralization, but this is not required by available structural evidence.

PETROLOGY AND GEOCHEMISTRY OF HOST ROCKS

Big Canyon-Type Deposits

Host rocks for gold deposits of the Big Canyon type were metamorphosed prior to ore emplacement, thus the first step in this study was to determine the composition of the metamorphic rocks. Metatuffs that are located more than 100 m from gold mineralization and considered to be unaffected by ore processes are medium green with millimeter-scale compositional layering that probably reflects original bedding because most of these rocks are not foliated (fig. 3A). The chief metamorphic minerals are epidote and amphibole, about 20–40 volume percent each, along with lesser amounts of plagioclase and calcite and minor quartz. Epidote is present as stubby grains 100–200) μm in size, and amphibole is highly prismatic (5:1 to 10:1, length to width), in grains as long as 100–500 μm, with yellow to green or yellow to blue-green pleochroism of actinolite or sodic actinolite. Calcite occurs in thin beds (<5 mm thick) in much of the basaltic metatuff; the carbonate is so widespread that it does not appear to be ore associated. Fine plagioclase (albite), generally less than 100 μm in size and untwinned, occurs between the epidote and actinolite in amounts as great as about 20 percent. Metamorphic albite is of finer grain size and more disseminated than albite that formed during ore-associated hydrothermal alteration. Hematite, which occurs in plates or elongate grains as long as 200 μm, is a common accessory (1–3 percent) as is sphene, which occurs in both coarse (300 μm) subhedral grains and fine grains or aggregates of fine grains about 20 μm in size. A few percent of pyrite is present in some little altered metatuffs that are located more than 100 m from mineralized structures.

Metadiorite occurs in drill core from the Big Canyon and Live Oak deposits. Metadiorite, which is similar in color to basaltic metatuff but is not layered, has distinctive plagioclase phenocrysts set in an aphanitic matrix, a texture that is retained by metamorphic minerals. Most of the metadiorite that I saw has a breccia texture with subangular fragments that generally are less than 2 cm in size. Sphene in metadiorite is like that in basaltic metatuff: aggregates of 20–40-μm microgranules that have no textural similarity to possible igneous Fe-Ti oxide minerals.

Alteration associated in time and space with gold is essentially one type with variations in texture and mineral proportions (fig. 3B–H). Pyrite, carbonate, and albite are abundant in this alteration, hence I will call it "PCA". These minerals formed by metasomatic processes by which S, CO_2, and Na were added to the rocks during both vein-filling and replacement reactions. This is mineralogically similar to propylitic alteration (Meyer and Hemley, 1967), but in these rocks there is abundant textural and chemical evidence for major compositional changes rather than weak hydrogen and carbonate metasomatism that usually is characteristic of propylitic alteration. The end product of most intense alteration is a granular tan albite-carbonate-pyrite rock with little resemblance to the prior rock other than content of Fe, Mg, Al, and Ti that have been reconstituted in newly formed minerals. A generalized sequential development of the alteration is apparent in adjacent samples collected at about 1-m intervals outward from the zones richest in gold or at centimeter scale in narrow mineralized zones in which the entire sequence from tan to green rock is present in a hand specimen. A first stage that is evident in thin section (fig. 3C), but not megascopically, is flooding by microgranular 10- to 30-μm albite with pyrite, sphene, apatite, and minor ankerite. Scattered coarser albite crystals in the microgranular matrix can produce a texture that resembles an albite porphyry (fig. 3G), but this probably is a metasomatic porphyroblast. A later stage, which is probably gradational in time or intensity, has much more carbonate that fills veinlets and replaces matrix albite; this stage is generally accompanied by coarser (100–300 μm) tabular crystals of albite that are twinned (fig. 3H). Crystals of apatite are present with the albite. A third, and possibly much later stage, is veinlets of carbonate that are distinctively white in hand specimen and effervesce strongly with dilute acid; these veinlets typically contain only coarsely crystalline calcite with no pyrite or albite.

Fe-Mg silicates show the effects of progressive PCA alteration. During early or weak PCA alteration actinolite tends to be modified to a variety with bluish pleochroism that is qualitatively indicative of sodic composition (riebeckite molecule). Hematite is present in many of these weakly altered rocks or in residual patches in which green color and prismatic amphibole texture are preserved. In later or more advanced stages of PCA alteration, actinolite can be present but is seemingly bleached to a nearly colorless variety, and in most everely altered rocks, which are most characteristic of large volumes of PCA-gold mineralization, there is no trace of the amphibole or its texture: no trace of original rock texture survives (fig. 3E–G). In these more advanced stages of alteration hematite is not present. Epidote occurs in some of the PCA alteration, but only as fine (<40 μm) inclusions in albite. Chlorite with dark-green color in transmitted light (Fe rich) forms in two stages: (1) early, in peripheral, weakly altered zones (fig. 3B), where it tends to be replaced by later carbonate minerals; and (2) late, with veinlets of calcite. Early chlorite might be a replacement of metamorphic epidote but does not replace amphibole.

Table 1. Statistical summary of major-element chemistry of metamafic rocks and metachert, Big Canyon area

[All values in percent, except Au, which is in parts per million. Normative minerals computed from chemical analyses: Q, quartz; Ab, albite, Carb, carbonate]

Variable	Metamafic rocks (N=57)					Metachert (N=24)				
	Minimum	Maximum	Mean	Deviation	Valid	Minimum	Maximum	Mean	Deviation	Valid
SiO_2	33.70	73.20	46.24	6.75	57	46.20	95.39	83.38	13.04	24
Al_2O_3	2.04	20.10	12.73	2.81	57	.69	19.30	3.61	3.66	24
Fe_2O_3	3.00	17.16	5.82	2.29	57	.32	12.01	3.65	3.42	24
FeO	1.65	9.43	3.20	1.25	57	.17	6.60	2.00	1.88	24
MgO	.13	10.60	5.01	2.29	57	.11	2.79	.90	.74	18
CaO	.05	15.00	7.86	3.84	57	.03	5.20	1.28	1.55	16
Na_2O	1.07	7.96	5.24	1.42	57	.23	4.37	1.18	.96	23
K_2O	.04	3.43	.58	.60	57	.04	.56	.25	.19	12
H_2O^+	.11	6.00	2.13	1.47	57	.11	10.00	1.17	2.02	24
TiO_2	.38	2.68	1.20	.50	57	.02	.94	.26	.25	24
P_2O_5	.06	1.45	.20	20	49	.05	.61	.25	.18	8
MnO	.03	1.55	.25	.27	56	.04	1.85	.58	.57	17
CO_2	.01	19.80	7.59	5.05	55	.01	7.77	1.77	2.66	16
S_{total}	.01	11.80	2.60	2.60	54	.02	8.61	1.70	2.61	22
Q	0.0	48.11	5.47	10.65	57	31.91	93.63	75.15	17.51	22
Ab	9.67	68.65	46.10	12.40	57	1.29	34.43	9.6	7.94	24
Carb	.02	42.97	16.58	11.42	57	.02	17.71	2.65	4.59	24
Au	.10	70.00	3.51	11.01	40	.02	8.61	1.70	2.61	22

Major-element chemistry (tables 1, 4) reflects the mafic character of the metamorphic rocks just described. These rocks are relatively rich in Fe, Mg, Ca, and Ti—generally similar to the composition of unmetamorphosed basaltic rocks. The best estimate of starting compositions, taken from 12 samples judged to have undergone little ore-associated metasomatism, suggests 45–55 percent SiO_2, 13–18 percent Al_2O_3, and 0.8–2.1 percent TiO_2 (all recomputed on a CO_2-H_2O-free basis), generally comparable to basalts (Le Maitre, 1976). Samples thought to be metamorphosed diorite or diabase have approximately the same composition as layered basaltic metatuff samples, certainly within the compositional variation caused by metamorphic and hydrothermal alteration. Hydrothermally altered rocks contain large amounts of Na, CO_2, and S; the percentages of normative albite and carbonate (the sum of normative calcite, magnesite, and siderite) range as high as 68 and 43 percent, respectively.

Titanium is useful as an indicator of rock parentage in cases of severely altered rocks with no relict minerals or textures. Altered rocks with more than 10 percent CO_2 tend to contain less than about 1.2 percent TiO_2, compared to about 1.8–2.1 percent TiO_2 in least altered mafic rocks. Most Ti resides in sphene, and some highly altered rocks contain rutile. Titanium probably has been reconstituted several times in these rocks. During regional metamorphism Ti migrated from sites in oxide and silicate minerals of igneous rocks to relatively coarse sphene greater than 100 μm with subhedral form. Microgranular aggregates of sphene formed during PCA alteration are nearly opaque; the individual crystals are less than 40 μm. In advanced stages of PCA alteration fine sphene is disseminated between grains of albite. There is nothing in the texture of sphene to indicate that it replaces igneous Fe-Ti oxides. Evidently Ti has migrated short distances (micrometers to millimeters) within the altered rocks but, on a bulk scale, has remained approximately constant except for zones of intense carbonate alteration that seem to have lost Ti.

Gold (determined by assay) is always associated with tan PCA-alteration zones. These zones are fracture controlled, but megascopic and microscopic features suggest they are mainly replaced rock rather than vein filling. A myriad of millimeter-scale veinlets at centimeter intervals form a stockwork that consists of about 90 percent altered wall rock and 10 percent vein. The tan PCA zones are thick (commonly 5–30 m), and commonly several PCA zones occur in a 100- to 200-m interval. Tan PCA zones are not everywhere enriched in Au, but in many drill holes gold assays for 0.3- and 0.6-m intervals of PCA are consistently greater than 1 g/t, with scattered intercepts that are much higher (10–70 g/t). According to correlation analysis (Davis, 1986) of the chemical data, gold correlates strongly with P, Fe, and Mn, but is independent of Na, CO_2, and S. The computed independence of Au with Na, CO_2, and S expresses the fact that albite, carbonate, and pyrite abundances are not proportional to Au content, despite the observation that Au is always associated with these minerals.
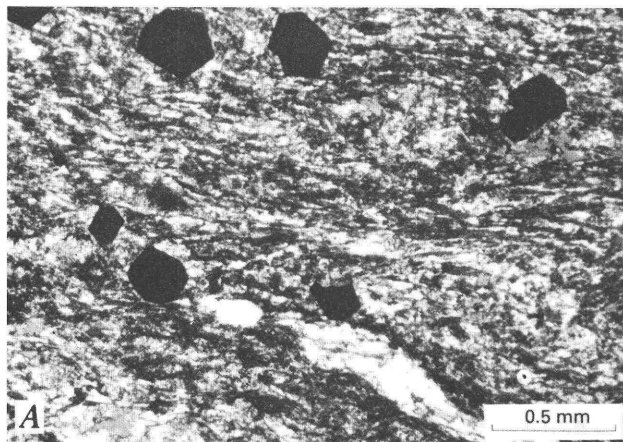
A, Layered, weakly altered actinolite-epidote-albite basaltic metatuff with scattered pyrite (black euhedral grains). Sample BC32–374, plane light.
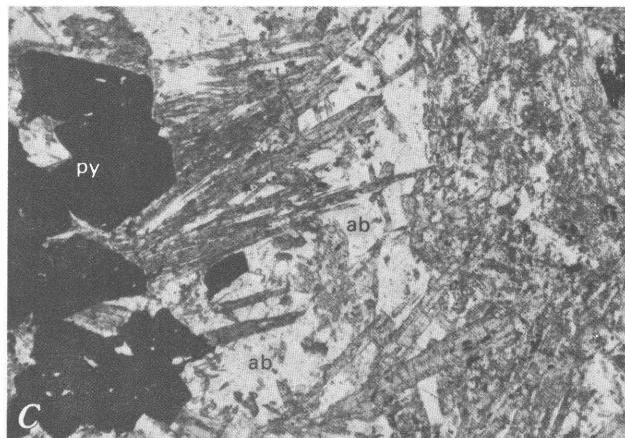
C, Moderately altered basaltic metatuff; acicular grains of actinolite survive in matrix of albite (ab) and pyrite (py). Sample BC27–226, plane light.
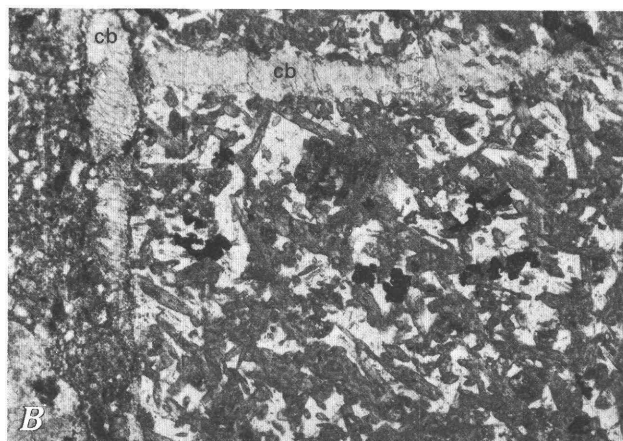
B, Incipient alteration along carbonate veinlet (cb); form of metamorphic minerals survives, but mafic minerals are replaced by chlorite. Sample BC27–206, plane light.
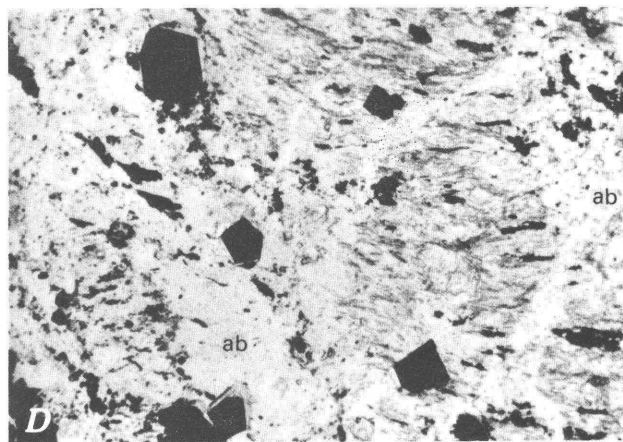
D, Highly altered basaltic metatuff; most of rock is albite (ab), but original character of rock is indicated by relict patches with acicular actinolite (right side) or strings of the fine sphene (left side, fine opaque grains). Sample BC16–101, plane light.

Qualitative estimates of changes in major-element composition during PCA alteration of mafic rocks are shown in table 2. Ideally, chemical changes are computed with knowledge of some constant parameter, such as volume or an immobile element like Al or Ti. For these highly altered mafic rocks I am not willing to assume that any element has been immobile, and it is very difficult to estimate the volume change during alteration. The computed values in table 2 are only rough estimates because changes in volume have not been included. These rough computations suggest that (1) Si is approximately constant; (2) Al, total Fe, Mg, K, Ti, and H_2O^+ are lost; and (3) Ca, Na, P, Mn, S, and CO_2 are added. These trends are in general agreement with inferences from chemical changes and petrography.

Vandalia-Type Deposits

Host rocks for Vandalia-type gold deposits are chiefly metachert, but some gold also occurs in adjacent basaltic metatuff. These rocks have been metamorphosed, and there is uncertainty as to whether gold was introduced before or after regional metamorphism. Recent near-surface oxidation has affected many of these rocks, most obviously producing clay and limonitic iron oxides. In many places gold values are high in fractured, oxidized zones, which suggests that there may have been some supergene enrichment of gold. Supergene oxidation also unlocked gold and permitted much easier recovery than from pyritic ores, which were not economic (Logan, 1938). basis.
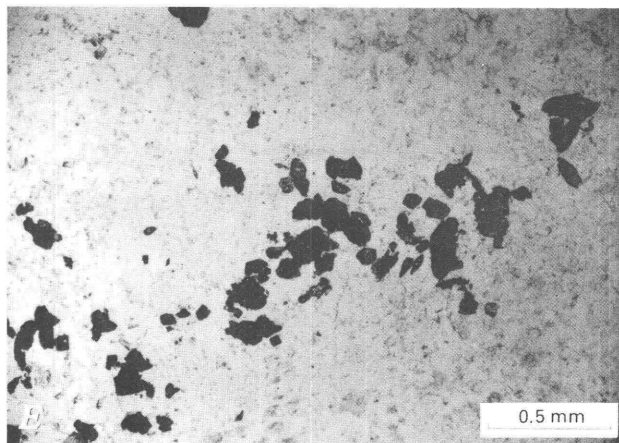
E, Albite-carbonate rock formed from basaltic metatuff; clusters of sphene (opaque) give a clue to protolith. Sample BC32–341, transmitted light.
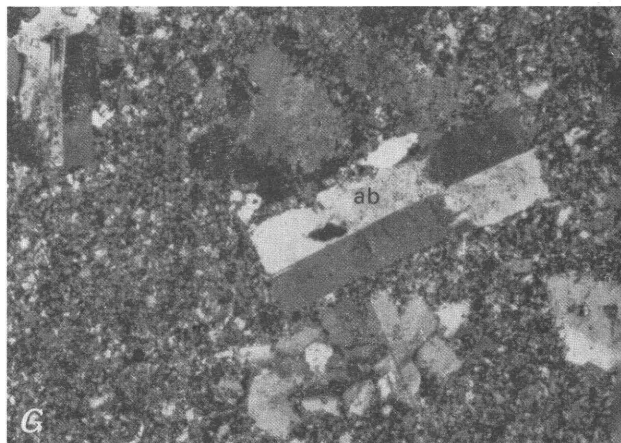
G, Albite alteration of basaltic metatuff with coarse and fine albite (ab); Fe-Mg silicates are destroyed. Sample 27–183, crossed polarizers.
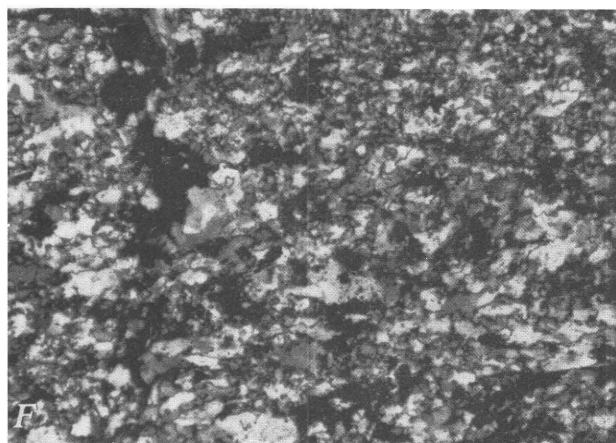
F, Albite-carbonate rock formed from basaltic metatuff; light-colored fine-grained rocks like this can resemble metachert in Vandalia sequence, but presence of abundant albite and sphene indicate that protolith of this rock was a basaltic tuff. Sample BC16–101, crossed polarizers.
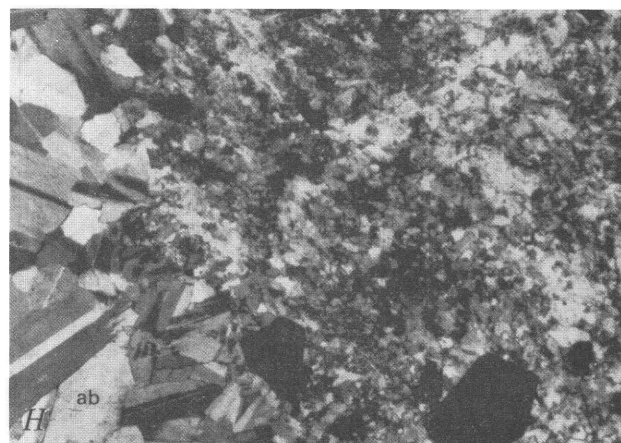
H, Albite alteration of basaltic metatuff in which early pervasive albite (ab), with disseminated pyrite, is very fine grained and cut by later coarse albite. Sample L07–86, crossed polarizers.

Figure 3 (above and facing page). Photomicrographs of altered mafic rocks, Big Canyon area. All photomicrographs taken in transmitted light.

Four facies can be distinguished in the metachert sequence: (1) chert, (2) pyritic chert, (3) chert with iron silicate, and (4) chert with iron oxides. The terminology of banded iron-formations (BIF) (James, 1954; Gross, 1980) can be used for some of these facies as long as the prefix "lean" is used because only rarely do the rocks contain more than 15 percent iron. Most of the metachert sequence is white or tan and contains less than 5 percent iron; it was derived from a "clean" chemical sediment with more than 90 percent silica. A small quantity is dark red to black, produces a red streak, and contains a few percent of fibrous riebeckite along with hematite; this could be termed lean silicate BIF (compare James, 1954) because total iron content is only 5–10 percent. The lean silicate BIF contains local "kicks" in gold but is not a host for large amounts of gold by either grade or volume. Finely layered metachert with laminae of iron oxides is interbedded with white metachert and in a few places contains more than about 20 percent total iron, thus this metachert could be called BIF. The majority of the BIF or lean BIF in the vicinity of gold mineralization is nonmagnetic by magnet or magnetic susceptibility test on core and outcrop. However, magnetic BIF forms a sequence more than 9 m thick about 1 km south of the Vandalia mine (R. Earhart, written commun., 1987). The part of the metachert unit of most interest for gold is the chert facies, which probably is a facies that was enriched in pyrite during chemical sedimentation or diagenesis as

Table 2. Chemical changes in alteration of mafic rocks

[Major elements are recalculated to a volatile-free basis, based on average compositions from 12 least altered and 20 highly altered samples]

Variable	Least altered (in percent)	Highly altered (in percent)	Percent change
SiO_2	49.60	49.57	0
Al_2O_3	15.88	12.51	−21
[1]Fe_2O_3	10.30	9.26	−10
MgO	7.49	4.92	−34
CaO	8.38	10.94	+31
Na_2O	4.87	6.24	+28
K_2O	0.93	0.43	−48
TiO_2	1.41	1.14	−19
P_2O_5	0.16	0.18	+12
MnO	0.22	0.27	+23
S_{total}	0.73	4.92	+573
[2]H_2O^+	3.41	1.04	−70
[2]CO_2	3.89	10.77	+177
[2]Au (in ppm)	0.15	2.16	+1340

[1]Total iron expressed as Fe_2O_3.

[2]Not recalculated to volatile-free basis.

postulated for pyritic BIF (James, 1954; and others). All these cherty rocks are finely laminated, and chert and pyrite layers are locally tightly folded in intraformational folds that seem to be soft-sediment features as might be produced in a sea-floor slump. No replacement or partial replacement textures involving pyrite and possible precursor sedimentary iron oxides have been seen. Tight narrow fractures coated by pyrite (or limonite after pyrite) are abundant, commonly about two or three per meter of core, and probably indicate remobilization of pyrite from earlier syngenetic sites.

Carbonate iron-formation is commonly interbedded with other facies of iron formation (James, 1954; Gross, 1980), and many large gold deposits elsewhere are associated with layered Fe-Mg carbonate that was interpreted to have formed as a volcanogenic exhalite (Ridler, 1971; Hutchinson and others, 1971; Boyle, 1979). All the large areas of Fe-Mg-carbonate rock in the Big Canyon area formed by alteration of mafic rocks; I saw no rocks that could be called carbonate iron-formation or carbonate exhalite.

Texture of the metacherts in thin section is distinctive. Quartz is the chief constituent and occurs in a tightly interlocked mosaic of 50–75 μm grains (fig. 4A). There is little or no evidence for clastic grains of quartz in these siliceous metasedimentary rocks. Fine laminae of white micas are evidence of former thin layers of clay, and small amounts of fine epidote indicate a calcareous component in the sediment. Hematite is present as fine plates about 20–50 μm long; fine sprays of riebeckite often radiate from the hematite. Titanium minerals such as sphene are rare to absent. The residence of about 1 percent Na_2O is not obvious in these fine-grained rocks; it might be partly in white mica, but most is probably
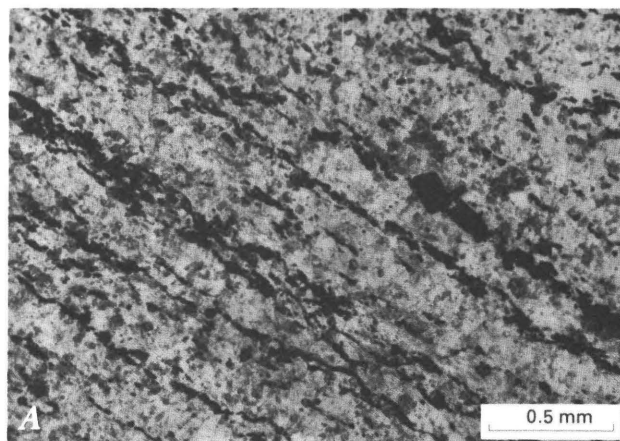
A, Typical finely layered pyritic metachert. Most of the pyrite is very fine grained and occurs along certain layers; some pyrite that is coarse grained reflects later hydrothermal or metamorphic processes. Carbonate (granular, high-relief grains) occurs in some layers. Sample BC2–132, plane light.
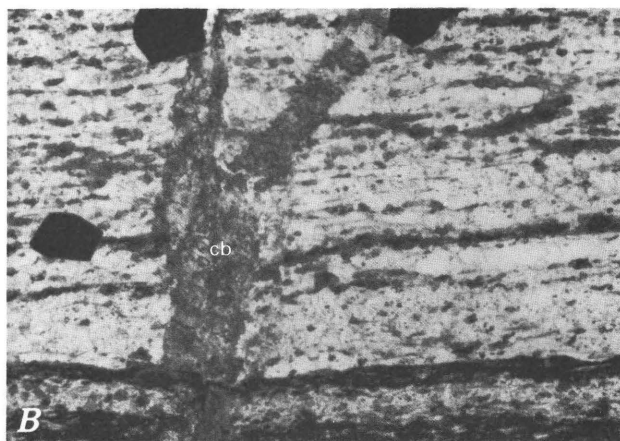
B, Carbonate vein (cb) cuts layers in metachert, and scattered fine rhombs of carbonate form in chert next to vein. Dark layers are fine pyrite, epidote, and actinolite. Sample BC10–111, plane light.

present as small grains of untwinned albite that have escaped notice.

Identification of alteration in metacherts that is associated with gold mineralization is not straightforward because of the fine grain size of most minerals. Some vein and replacement textures that include carbonate, albite, and pyrite (fig. 4B–E) suggest a postmetamorphic stage of superimposed alteration. It is difficult or impossible to distinguish between metamorphic redistribution and postmetamorphic introduction of components. If the gold (or other elements) was deposited with pyrite early in the history of the chemical sediments, then it would have been present during metamorphism and postmetamorphic alteration. In this scenario gold would logically be recrystallized and possibly mobilized a short distance
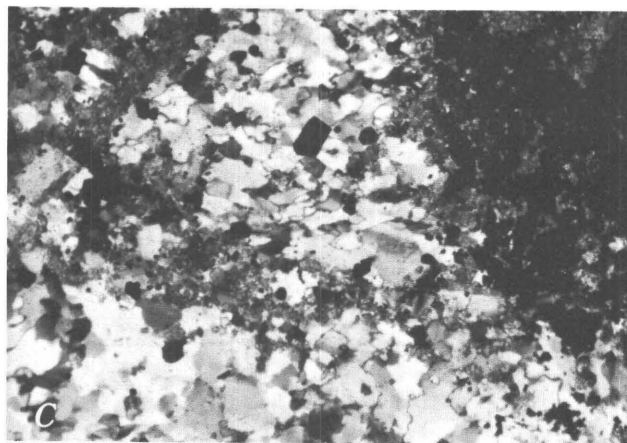
C, Pyrite-carbonate-albite alteration (right side) recrystallizes layered metachert in a zone of fractures. This alteration is thought to be postmetamorphic. Sample BC10–113, crossed polarizers.
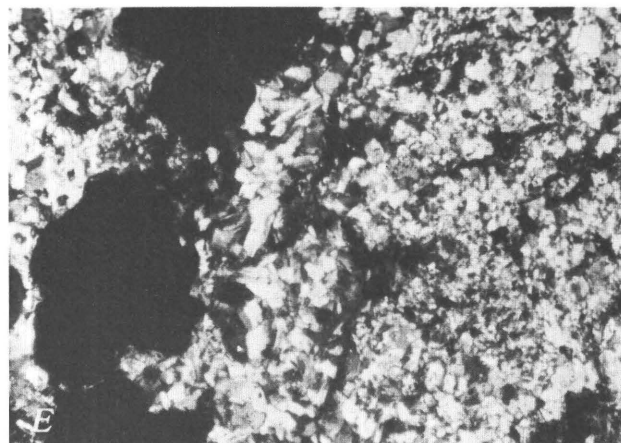
E, Albite-altered rock, the protolith of which probably was a chert. Rock is rich in gold and pyrite; most of the latter is discordant to bedding and seemingly added along with albite. Sample BC10–60, crossed polarizers.
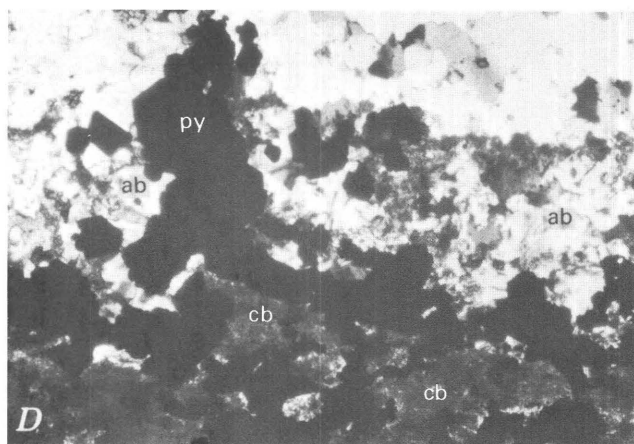
D, Pyrite-carbonate-albite replaces metachert; the pyrite (py) is in fractures that are obvious in core, but the carbonate (cb) and albite (ab) are most clearly shown by chemical analyses and thin sections. Sample BC10–73, crossed polarizers.
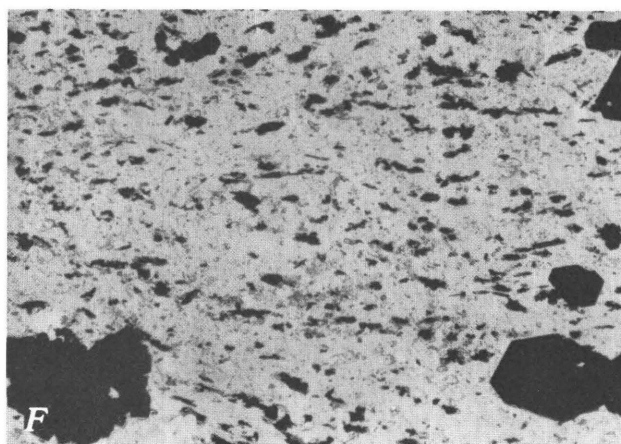
F, Albite-rich rock, the protolith of which probably was a basaltic tuff. Although this interval of core is finely laminated and very light in color (originally thought to be metachert like the rocks above it in core), the abundant fine sphene and rutile (opaque, seemingly along beds) and albite suggest that its protolith probably was a mafic volcanic rock. Chemical analyses show its composition is much closer to basalt than to chert. Sample BC10–63, plane light.

Figure 4 (above and facing page). Photomicrographs of metachert and alteration in metachert. All photomicrographs taken in transmitted light.

during metamorphism; this seems to have happened to pyrite (fig. 4*A*). Sodium and carbonate enrichment in metacherts is probably postmetamorphic, as suggested by textures of some samples (fig. 4*C*–*D*), thus might be considered to have been overprinted on earlier(?) gold. This cannot be proven or disproven by textural relations among the fine-grained minerals or by bulk chemical analyses that cannot discriminate among minerals of different ages. However, in later sections of this report it will be argued that structural evidence and geochemical associations are most consistent with postmetamorphic introduction of gold and other elements at the same time as in the nearby Big Canyon deposit.

The major-element composition of 24 samples of metachert (tables 1, 4) is consistent with the predominance of quartz in these rocks. Concentrations of

Mg, Ca, K, and Ti generally are very low, but total iron (expressed as Fe_2O_3) ranges to more than 20 percent. Contents of Na and Al are higher than expected of "clean" metacherts; computed normative albite ranges as high as 34 percent and averages 9.6 percent. In most samples the amount of Na is close to that in stoichiometric balance with Al to make albite; this is interpreted to mean that during sodium metasomatism Na was deposited only to the extent that it could combine with Al

already present in the metasedimentary rocks to form albite. Content of Au in the metachert samples correlates most strongly with Al, strongly with FeO and Fe_2O_3, and moderately with Ti, P, and S.

Problematic Alteration in the Vandalia Sequence

There are at least four lithogeochemical problems for rocks of the Vandalia sequence that bear on the question of the age and character of the Vandalia gold mineralization. These problems are: (1) the composition of beds that seem to represent sedimentary mixing of tuff and siliceous chemical sediment, (2) the enrichment of Al-Na-Ti in metacherts, (3) the textural and chemical evidence for postmetamorphic addition of carbonate and albite to metacherts, and (4) the sodic and carbonate alteration of diabase dikes in metachert. These problems can be reduced to two fundamental questions regarding (1) the relative ages and structural relations of chert and basaltic tuff and (2) the relative age and influence of carbonate-albite alteration on the metachert sequence.

The metachert sequence is in fault contact with basaltic metatuff according to the interpretations of Earhart (1988), and there is substantial evidence for this. This relationship is consistent with the vastly different compositions of the two units and with the presence of fractures at the lithologic contact. However, relations in most of the 16 drill holes in the northwestern part of the study area (fig. 2) are not entirely consistent with this interpretation. All 16 drill holes intersect both metachert and basaltic metatuff sequences, and most of the holes display alternating 1–3-m-thick layers that seem to represent interbedding because there are no breccias or changes in bedding attitudes suggestive of faults. Basaltic metatuff adjacent to the thick section of metachert is commonly fractured, but this seems to reflect deformation next to a rigid body during folding rather than the presence of a fault. PCA alteration is developed in both metachert and basaltic metatuff in the vicinity of some of these contacts (fig. 4E–F) as seen in thin sections, but this is not evident megascopically. However, it must be noted that there is a general problem that some faults are not prominent in drill core. In addition, diagenesis or metamorphism might have healed or obscured the faults, which would make them especially difficult to recognize in core.

Some bedded rocks that were sampled for chemical analysis (about 0.3-m-long sections of core) have chemical compositions intermediate between normal metachert and balsaltic metatuff: SiO_2 is 55–80 percent, Al_2O_3 is 2–10 percent, Na_2O is about 2–5 percent, and TiO_2 is greater than about 0.3 percent. In thin section these rocks have unusual textures that seem to be similar to metatuff in parts of the thin section and more like metachert a few millimeters away. The presence of high concentrations of Al and Ti in samples with the texture of a chemical sediment is hard to explain by any mechanism other than mixing with a tuffaceous component because Al and Ti seem to be quite immobile in epigenetic processes in these rocks and elsewhere.

Fine-grained diabase dikes that cut metachert have major-element compositions that are generally similar to the basaltic metatuff, which would be logical if the dikes are roughly contemporaneous with the basaltic metatuff. Also, the dikes provide another time reference for alteration. They are strongly enriched in Na and CO_2, which I interpret as indicating that the alteration of the dikes occurred at the same time as the PCA alteration along the Big Canyon fault zone.

Carbonate minerals vein the metachert sequence and PCA alteration is developed at many locations in 11 of the 16 northwestern drill holes. Many of these PCA alteration zones contain anomalous Au, and in some intercepts the Au exceeds 1 g/t. The formation of gold mineralization of both Vandalia type and Big Canyon type less than 100 m apart vertically, as seen in drill holes 4, 10, and 32, is most easily explained as one event.

ORE PETROLOGY

Opaque minerals were examined in fair detail in reflected light at magnifications from 40× to 1,000× to gain information on their identity and paragenesis. In most cases the ore minerals are very fine grained (less than 100 μm) and disseminated in the rock matrix, thus the time of their formation is not as easily determined as for vein-filling minerals.

Arsenopyrite.—Arsenopyrite is reported to occur with gold in the Big Canyon mine (Clark and Carlson, 1956). Such an occurrence would seem likely in these ores, but it has not been confirmed in these petrographic studies. The shape and optical properties of arsenopyrite are similar to those of pyrite, and consequently arsenopyrite could have been missed. Concentrations of about 1,000 ppm As, which are found in many rocks in this study, could produce just a few grains of arsenopyrite per thin section. Alternatively, the As could be in the pyrite lattice as demonstrated by microprobe studies of pyrite from Carlin-type gold deposits in Nevada (Wells and Mullins, 1973), but this may not be an appropriate analog for these deposits.

Gold.—Native gold has been identified in 26 polished sections using reflected-light optical methods. About 50 grains have been identified with confidence (fig. 5), and an equal number were located although their small grain size (<1 μm) did not permit positive identification. Most of the identified gold grains are in PCA-altered mafic rocks (24 samples). Only two samples of metachert contained gold grains large enough to

permit reliable identification, but grains smaller than 1 μm and suspected to be gold were observed in several other samples of metachert. Pyrite was present in all the gold-bearing samples, but gold occurred as inclusions in pyrite in only three samples (fig. 5). Most gold that I recognized in reflected light occurs in the matrix between grains of albite or albite and carbonate. Based on microscopic features and correlation of gold assays and alteration, it is evident that gold occurs chiefly with albite-pyrite or albite-carbonate-pyrite flooding and veining of mafic rocks that are tan or medium gray. The texturally late calcite-chlorite veins do not appear to have much gold. The native gold in the PCA-altered mafic rocks is relatively coarse grained; most grains are 2–8 μm, but some are as coarse as 30 μm. Some gold grains

probably are less than 1 μm, but their identity requires confirmation.

Gold is difficult to locate in samples of metachert. Only a few grains larger than 2 μm could be spotted; about 25 grains smaller than 1 μm had color that was more yellow than pyrite, but these could have been chalcopyrite. Samples of metachert that contain microscopic gold and most samples of metachert with assays >1 ppm Au have textural or chemical indications of added albite ± carbonate as well as pyrite and are enriched in the same trace elements as the PCA-altered mafic rocks.

Hematite.—In this study the term hematite is reserved for hard, crystalline iron oxide with red internal
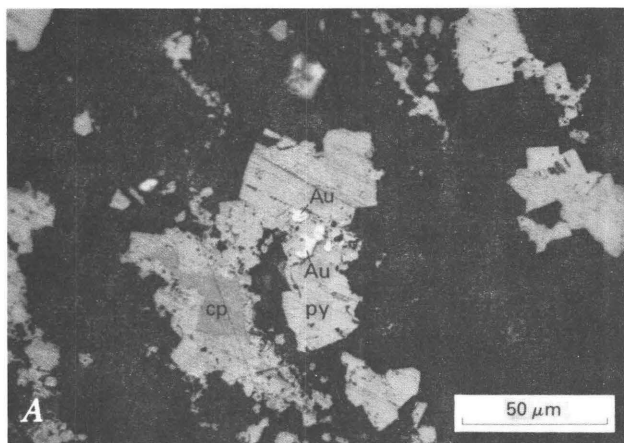
A, Gold (Au) with pyrite (py) and chalcopyrite (cp), enclosed in albite-carbonate gangue (black). Sample L07–59.
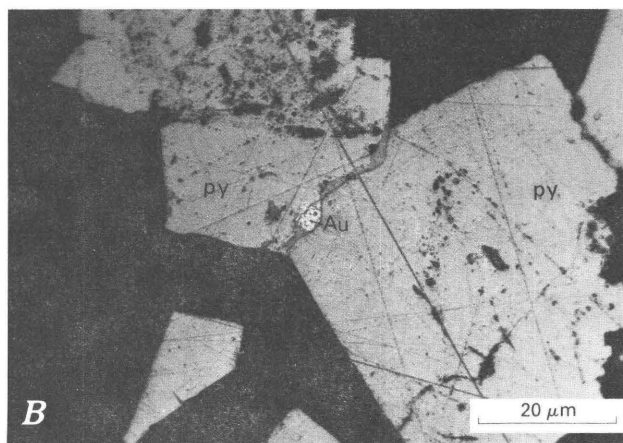
B, Gold (Au) on grain boundary of pyrite (py), enclosed in albite-carbonate gangue. Sample L07–59.
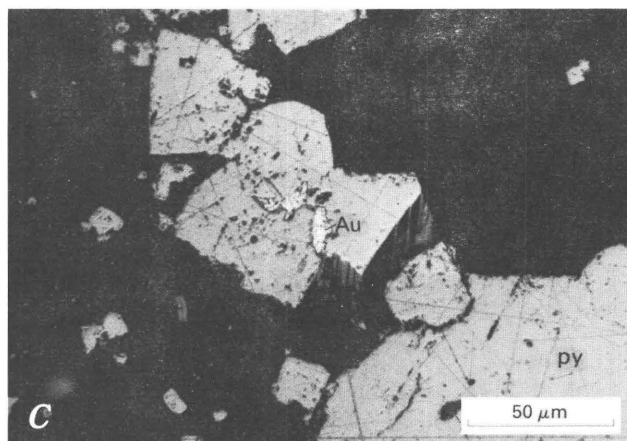
C, Gold (Au) in pyrite (py), within albite-carbonate alteration of basaltic metatuff. Sample BC29–167.

Figure 5. Photomicrographs of gold associated with pyrite. Photomicrographs taken in reflected light with oil-immersion lenses.

reflections, thereby eliminating iron oxides in the weathered zone. In both metachert and metabasaltic rocks of this area hematite is generally tabular or platey in form and less than 100 μm in length. In metacherts hematite is generally oriented with plates parallel to bedding, and fine needles of riebeckite commonly radiate from the hematite. The texture of hematite in metacherts is consistent with its formation as part of a chemical sediment, with only minor textural change in metamorphism. Hematite also occurs in amounts as great as about 1 percent in some of the less altered mafic igneous rocks. It appears to form along with epidote (a ferric iron mineral) and actinolite in regional metamorphism. Hematite is not present in most hydrothermally altered mafic rocks but is present in some local parts of thin sections that have retained much of their metamorphic texture, mineralogy, and green color. There is no evidence for partial replacement of hematite by pyrite, and pyrite does not mimic the platey form of hematite. Thus, in the hydrothermal alteration of mafic rocks of this area it appears that if hematite was produced in the rock by metamorphism it subsequently was dissolved and the iron was redistributed into hydrothermal sulfide, carbonate, or silicate minerals.

Magnetite.—Magnetite generally is absent from these rocks but locally is abundant in magnetic BIF sequences south of the Vandalia mine. According to magnetic susceptibility measurements and petrographic studies, magnetite is not present in most of the metachert sequence near the Vandalia mine. Magnetite is present in a few samples of slightly altered metadiorite or metabasalt from the Big Canyon and Live Oak deposits. In those metamorphic rocks the magnetite is present as subhedral equant grains 50–100 μm in size. A few of the grains abut pyrite, which suggests possible replacement by the sulfide, but most pyrite in these mafic rocks is coarser than the magnetite and does not show direct evidence of having replaced former magnetite.

Sphene and rutile.—Although not always considered to be "ore" minerals, sphene and rutile will be described here because they have been studied in detail as indicators of probable mafic rock precursors. Titanium in these rocks resides predominantly in sphene and rutile rather than in Fe-Mg silicates. Sphene formed during metamorphism, and it probably was redistributed during hydrothermal alteration. Most sphene is anhedral and very fine grained (less than 50 μm). It is translucent to nearly opaque and is generally brown in transmitted light. In reflected light with high-magnification oil-immersion objectives, sphene has bright white to brownish-red internal reflections because of its high dispersion. In reflected light this sphene, which often looks like sugar, is very distinctive while making high-magnification scans for gold. At high magnification with reflected light most sphene is observed to be an aggregate of many microgranular crystals in an anhedral mass about 100–200 μm in size. In a few metadiorites the sphene aggregates take on a boxwork form that resembles ilmenite lamellae in Fe-Ti oxides, but in most samples sphene has no specific morphology to suggest formation by replacement of a former Ti-bearing mineral. In highly altered rocks that are characterized by albite and carbonate, sphene tends to occur as 20–40-μm microgranular single or multiple grains in albite (fig. 3F) and locally as closely spaced grains that appear to be in a veinlet. In foliated rocks, sphene tends to be in clots or aggregates that line up on foliation; mechanical shear may have caused the tiny grains to aggregate. At high magnification, in which the microscope focuses inside the thin section rather than on its surface, tiny (less than 5 μm long) needles of a honey-colored mineral can be seen to grow from some sphene surfaces—the needles are thought to be rutile or anatase (TiO_2 polymorphs). Sphene is present in small amounts in metacherts.

Rutile is present in some highly altered mafic rocks where it can exceed sphene in abundance (1–3 percent). Rutile is honey colored in convergent transmitted light and is gray with medium reflectivity in reflected light. Where crystals are 100–200 μm in size they are prismatic, and striations can be seen on the prism faces when observed with high-power oil-immersion objectives and reflected light. As mentioned above, some rutile seems to form from corroded sphene, but most is isolated in a silicate matrix and shows no textural indications of parentage. Rutile is supposedly rare in metamorphic rocks and possibly is formed only under conditions of unusually high CO_2 partial pressures (Schuiling and Vink, 1967). The textures of both rutile and sphene suggest that titanium has been mobile locally in these rocks during metamorphism and hydrothermal alteration, but near constancy of TiO_2 contents for most altered rocks suggests that the titanium has not moved more than a few millimeters.

Chalcopyrite.—A characteristic feature of these ores is the low content of base-metal sulfide minerals. The only one that is observed in many samples is chalcopyrite, but it is never more than a trace constituent. Chalcopyrite occurs chiefly in altered mafic rocks as 5–20-μm grains that at first glance (at 400 × magnification) resemble gold. Some chalcopyrite occurs as inclusions in pyrite.

Pyrrhotite.—A tan sulfide occurs as small inclusions in the cores of pyrite. This phase is not as anisotropic as most pyrrhotite that I have studied from other deposits, but this estimate may be caused by the very small size (< 20 μm) of these grains. Pyrrhotite is reported to occur in the Big Canyon deposit (Clark and Carlson, 1956), but from my research it does not appear to be abundant. The lack of magnetism in the sulfidic ores as measured by a

sensitive magnetic susceptibility meter also indicates little or no pyrrhotite is present.

Pyrite.—Pyrite is an important mineral in these gold deposits as it constitutes a visual guide to potential gold zones. Pyrite is present in all rocks that contain gold at concentrations greater than about 0.1 ppm, except in the weathered zone where gold is associated with limonitic iron oxides derived from pyrite. The formation of pyrite is probably directly or indirectly involved in gold precipitation.

Pyrite is present in metachert in amounts as great as about 10 percent. Pyrite in the metachert occurs both on bedding planes, as indicated by layers rich in other minerals such as riebeckite, epidote, or hematite, and on fractures. Perhaps the best evidence for a syngenetic or diagenetic origin for some pyrite is its occurrence in layers that are folded or swirled in intraformational structures that almost certainly formed while the sediment was unconsolidated. There is no textural evidence for pyrite replacing a sedimentary iron oxide in these swirled beds. Also, there is some regularity and predictability in the stratigraphic occurrence of pyritic metachert as mapped by Gold Fields Mining Corp. personnel (Osterberg and others, 1984), although three-dimensional information from outcrop and drilling is not sufficiently detailed to permit reconstruction of likely facies changes that include pyrite, hematite, and magnetite in the chemical sediment. Because of the tiny grain size of gold that has been observed in metacherts, no reliable paragenetic relation can be defined for gold relative to pyrite; ambiguous relations can easily be attributed to very local mobilization during metamorphism or possible postmetamorphic processes. I assume that much of the sulfide in the metachert sequence was a product of diagenesis, and that some probably was remobilized into fractures.

Pyrite also is widespread and abundant in mafic rocks other than serpentinite. Pyrite content is locally in excess of 10 percent in fractured and altered mafic rocks, but most commonly pyrite content is about 3–5 percent. Pyrite in the mafic rocks tends to be somewhat coarser than in the metacherts, with some grains in excess of 1 mm, but grains finer than 100 μm are not uncommon. Pyrite in these rocks is euhedral to subhedral. Pyrite grains coarser than about 200 μm tend to have inclusions of silicate minerals, and the cores of some have tiny grains of a tan (in reflected light, oil immersion) mineral that resembles pyrrhotite. The grains of pyrite almost always are coarser than any magnetite or hematite seen in the mafic rocks, no pyrite has the form of the iron oxides, and no composite grains of pyrite plus iron oxide are seen—these features are evidence that pyrite does not form as a direct replacement of preexisting iron oxides in the mafic rocks. Pyrite is invariably accompanied by albite or carbonate in the mafic rocks, either

flooding the rock or filling veinlets. Late calcite ± chlorite veinlets tend to have little pyrite. Some pyrite is weakly anisotropic, but the cause or significance of this for this occurrence is not known.

MINOR–ELEMENT GEOCHEMISTRY

Minor-element geochemistry of 82 samples is summarized in table 3. The most distinctive feature about the results of the minor-element geochemistry is the low content of base metals, such as Cu, Pb, and Zn, and the very low content of Ag, which was detected in only three samples (maximum concentration of 34 ppm). Considering that most of the samples were picked as being mineralized with several percent of pyrite, a higher content of chalcophile elements might have been expected. The one very high concentration of Mo (14,000 ppm) seems out of line and may reflect contamination by MoS_2 in grease used on drilling equipment. Concentrations of the "mafic" suite of elements Co-Cr-Ni-Sc-V are quite high and seem to reflect the mafic character of the metamorphic host rocks, as will be described further in the next section. Arsenic is highly enriched in Au-bearing samples. In general the minor-element composition of altered rocks from the Big Canyon and Vandalia deposits conforms to the pattern of enrichment in rare metals but not base metals that was described by Kerrich (1983) for Archean gold deposits of Canada. The rare elements and REE (rare-earth elements) emphasized by Kerrich are enriched with Au in these deposits as summarized in table 3. All results for Bi are < 10 ppm (lower limit of detection), and W could not be determined by the ICP method. Qualitative REE patterns (based on only five elements) for altered and Au-rich samples are flat with enrichments of about 10–100 times chondrite values; similar patterns were reported by Kerrich (1983).

Factor analysis (Davis, 1986) of the minor-element data for all 82 samples suggests some element associations: (1) rare-earth elements—Eu, Nd, Yb, Y, Ce, and La; (2) mafic group—Cr, Ti, Ni, Co, Sc, and Y; (3) base-metal group 1—Mo, Pb, Hg, Sb, and Te; (4) base-metal group 2—Zn, V, Cu, Mn, Fe, S, and As; (5) P–Au with no other associated elements according to this analysis; (6) Ba-K, possibly as K-feldspar or white mica?; and (7) Se-As-S—of uncertain age and mineralogy. When major elements were included in a factor analysis, the group Ca-Sr-Na was indicated to be associated with CO_2, whereas Mg was indicated to be associated with the mafic group (2 above). There are many geologic, mineralogic, and age explanations of these statistical associations, but they are useful for directing attention to groups of elements in the large dataset. For instance, do the compositions of the two base-metal groups (3 and 4

Table 3. Statistical summary of minor-element chemistry of altered rocks, Big Canyon area

[All values in parts per million. ---, no data (none detected)]

Variable	Mafic rocks (n = 57)				Metachert (n = 25)			
	Minimum	Maximum	Mean	Valid	Minimum	Maximum	Mean	Valid
Ag................	2.0	34.0	12.4	5	---	---	---	0
Au................	.10	70.0	3.5	40	0.1	9.0	1.8	7
As................	.9	2700.0	409.5	57	3.8	3300.0	469.9	25
Ba................	8.0	6200.0	280.0	57	11.0	1200.0	262.7	25
Co	2.0	100.0	40.2	57	1.0	75.0	14.5	24
Cr................	8.0	800.0	251.3	57	4.0	210.0	28.6	25
Cu	5.0	630.0	77.5	57	14.0	1000.0	135.9	25
Ga................	10.0	37.0	20.0	57	4.0	27.0	9.5	25
Hg................	.02	6.3	.40	54	.03	1.2	.29	23
Li.................	2.0	59.0	18.6	50	2.0	14.0	6.0	16
Mo	2.0	14,000.0	988.6	18	2.0	480.0	70.8	9
Ni................	14.0	390.0	157.3	57	4.0	250.0	45.1	25
Pb................	4.0	570.0	56.6	13	4.0	43.0	12.8	16
Sc	9.0	50.0	28.6	57	2.0	65.0	9.2	25
Sr................	10.0	680.0	235.7	57	3.0	140.0	39.0	22
Sb	.1	69.0	3.8	57	.2	11.0	2.5	25
Se	.10	18.0	2.3	38	.3	11.0	2.8	10
Te................	.02	22.0	.86	44	.04	2.6	.47	25
V	49.0	490.0	225.5	57	10.0	870.0	125.6	25
Zn	22.0	190.0	73.0	57	6.0	340.0	66.9	24
Ce................	4.0	65.0	16.2	49	8.0	96.0	22.0	25
Eu	2.0	3.0	2.3	3	3.0	6.0	4.5	2
Ho................	5.0	5.0	5.0	1	---	---	---	0
La................	2.0	80.0	13.7	31	6.0	140.0	24.6	25
Nd	4.0	75.0	13.6	48	5.0	150.0	22.6	25
Y	4.0	50.0	16.3	57	2.0	59.0	10.3	21
Yb	1.0	4.0	2.0	50	1.0	8.0	2.8	6
Th................	6.0	9.0	7.4	5	4.0	8.0	6.0	5

above) indicate that there were two stages of sulfide deposition in time and space? This is not evident in the petrology of the deposits.

The minor-element signatures of the two deposit types are different for elements that seem to reside in rock-forming minerals but similar for elements that are associated with Au. Keeping in mind the mafic character of the rocks in the Big Canyon-type deposits, it is not surprising that Ni, Co, Cr, V, and Sc have higher concentrations in those rocks, whereas La, Ce, Nd, and Eu have higher concentrations in the metachert suite of samples. The elements listed are statistically different between the two groups of samples and are reliable for distinguishing the two types of deposits when using a method termed "discriminant function analysis" (Davis, 1986). The concentrations of Sr, Li, and Ga are significantly higher in the metamafic (Big Canyon) rocks and presumably reflect an association with aluminosilicates (albite). Concentrations of As, Hg, Sb, Se, and Te are not significantly different between the two groups of samples. Likewise chalcophile elements Cu, Pb, and Zn are not significantly different in the two groups. The fact that the content of probably ore associated "pathfinder"

elements, such as As and Se, and of chalcophile elements, is not systematically different in the two types of gold deposits may be an indication that the mineralization is more similar than dissimilar.

Multivariate statistical tests of element associations with Au suggest that P, As, Ce, La, Nd, and Eu have significant positive associations, whereas some other elements that are suspected to be associated with Au, such as Hg, Sb, Se, Te, S, and Na, have only weak positive associations. The suite of elements associated with Au is the same for both deposit types as indicated by correlation analyses run on 25 Vandalia-type samples and 57 Big Canyon-type samples. For both deposit types the association of Au with P and REE is significant. The unsuspected Au-P association is a reminder that apatite is a prominent accessory mineral in the albitic alteration zones. Two differences were indicated when comparing Au associations in the subgroups: in the Vandalia subgroup of samples Au has strong positive associations with S ($r = 0.64$) and Na ($r = 0.22$), whereas in the Big Canyon subgroup Au is independent of S and Na ($r = 0.05$ and -0.02, respectively). The small correlation coefficients of Au-Na and Au-S do not seem consistent

with petrographic observation but probably are correct as a reminder that many altered rocks in the Big Canyon-type deposits have pyrite and albite but do not contain much Au. The computed positive associations of Au-Na and Au-S in the Vandalia subgroup of samples are consistent with petrographic features.

Arsenic is enriched in these altered rocks and is associated with Au. The residence of As is not a simple problem. The highest concentrations of As (1,100–3,300 ppm) are in near-surface, oxidized, limonitic samples that presumably contain an arsenate mineral such as scorodite. Many pyritic samples contain 500–1,000 ppm As, and six contain 1,100–2,700 ppm As; this amount of As would logically reside in arsenopyrite but might be in the pyrite lattice. If total S and As results are recomputed in terms of pure pyrite, much "pyrite" would contain about 2 weight percent As, and a few samples suggest a "pyrite" with as much as 6 weight percent As. Microprobe analysis, which can detect less than 1 percent As in pyrite, should be undertaken to test the residence of As in the sulfidic rocks.

DISCUSSION

Big Canyon-Type Deposits

Character of Deposits

The Big Canyon deposit and other similar prospects in the study area, such as the Live Oak, are structurally controlled vein or stockwork deposits. These deposits formed after the peak of regional greenschist-facies metamorphism because those metamorphic minerals are altered along the gold-bearing structures. The maximum geologic age for the gold mineralization is Late Jurassic, which is the age of the Logtown Ridge Formation that is cut by the Big Canyon fault and that contains local alteration and minor gold. The Big Canyon-type deposits are characterized by intense alteration of mafic rocks that results in alteration and vein filling composed of albite, carbonate, and pyrite; this PCA alteration grades outward to chlorite-carbonate-pyrite alteration. Gold is intimately associated with the PCA veining and flooding. Base metals such as Cu, Pb, and Zn are only slightly enriched in the gold zones, but As and REE, and to a lesser extent Hg, Sb, Se, and Te, are enriched along with Au.

A different age and setting for the Big Canyon-type deposits are favored by the Gold Fields Mining Corp. exploration geologists (Osterberg and others, 1984; M. Osterberg, written commun., 1987). They interpreted the structure, especially at the Live Oak prospect where they drilled 15 core holes, as that of a pipe that formed during Paleozoic mafic volcanism in a manner similar to foot-wall feeder structures below massive sulfide deposits. The structure and associated carbonate alteration are thought to be low-pressure, synvolcanic processes. From my more limited knowledge of the Big Canyon zone of mineralization, I can see two major problems with this hypothesis: (1) The mineralized structures appear to be part of the Big Canyon fault zone; and (2) the PCA alteration is, in my opinion, superimposed on metamorphic assemblages rather than being synvolcanic (premetamorphic). Multistage genesis, including postmetamorphic remobilization, might reconcile the premetamorphic and postmetamorphic origins favored by Gold Fields Mining Corp. geologists and by me, respectively, but I do not have evidence in support of this and it will not be considered further.

Comparison With Other Gold Deposits

The Big Canyon-type deposits are generally similar to gold deposits of the famous Mother Lode and Allegheny districts of California (for example, Knopf, 1929; Ferguson and Gannett, 1932; Landefeld and others, 1986). The carbonate alteration, and associated albite and pyrite, are very similar, although Cr-mica (mariposite) and muscovite are more abundant in the Mother Lode deposits. Albite is locally abundant in Mother Lode deposits (Knopf, 1929), but it does not seem to be as widespread or abundant there as it is in the Big Canyon-type deposits. The structural style of the Big Canyon-type deposits may be similar to some Mother Lode deposits that tend to be localized on second-order structures associated with the Melones fault zone, rather than with the major structure (Knopf, 1929; Ferguson and Gannett, 1932). A big difference is the lack of abundant quartz vein filling at Big Canyon; the Mother Lode veins are dominated by quartz of many generations that fills veins tens of meters wide (Knopf, 1929). The Mother Lode deposits have low base-metal content but are enriched in As.

The Big Canyon-type deposits are arguably similar to some Archean gold deposits of the world that have associated carbonate alteration and occur in mafic igneous rocks (Hutchinson and others, 1971; Boyle, 1979; Hodgson and MacGeehan, 1982). In making this comparison it is important to exclude those deposits thought to be in or associated with carbonate exhalites, because there is no evidence for layered, exhalitive carbonate rocks in the Big Canyon area, regardless of the debate over the origin of Archean carbonate rocks in Canada, Australia, and other parts of the world. Very similar "gold-only" deposits in metamorphosed Archean mafic igneous rocks occur at Yellowknife, Northwest Territories (Boyle, 1979), Sigma mine, Abitibi Belt,

Quebec (Robert and Brown, 1986), and Golden Mile, Kalgoorlie, Australia (Phillips, 1986). In addition to differences in age and structural setting, these examples have more potassic (muscovite) alteration (with minor albite or albite replaced by muscovite) than does the Big Canyon deposit.

Exploration Significance

Exploration and resource assessment of Big Canyon-type deposits can utilize several features that were previously described: structural control, PCA alteration, and minor-element signature. The most general feature is structural control by the suture that separates the Mother Lode belt from the Melange belt (locally the Big Canyon fault) and by secondary faults that splay from the Big Canyon fault. Mafic rocks cut by these faults should be examined for PCA alteration and enrichment in Na, As, or rare metals. Gold may be the best guide to gold deposits, but alone would not be diagnostic of the Big Canyon-type of deposit. There is a high potential for the existence of additional deposits like the Big Canyon, but discovery of such deposits may be extremely difficult because of poor exposure or cover by younger materials.

Vandalia-Type Deposits

Character of Deposits

The Vandalia gold deposits are associated with pyritic and pyritic-hematitic metachert that formed as a chemical sediment (exhalite); some of the Vandalia gold also seems to occur in silicified basaltic metatuff. Questions remain about the formation of these ores. First, is the metachert sequence exotic relative to the adjacent basaltic metatuff, or did it form as part of the volcanic sequence? Second, did the gold form as part of the chemical sediment or was it introduced much later, following metamorphism, at the same time as the Big Canyon mineralization? These two problems are not necessarily related. There is little doubt that the chert formed as a chemical sediment, and the presence of several percent aluminum in nearly all samples suggests that there was a pelitic or volcanic component in the sediment. The origin of beds with compositions intermediate between chert and tuff (SiO_2, about 60–75 percent; Al_2O_3, 5–10 percent) is not clear—the most likely processes are (1) mixing and diagenetic alteration of tuff and siliceous exhalite, and (2) postmetamorphic hydrothermal alteration. Because some of these beds contain substantial amounts of titanium, which is thought to be relatively immobile in hydrothermal processes, and

because silica does not seem to have been added in most of the hydrothermal alteration in the Big Canyon area, I prefer to explain the origin of these intermediate composition rocks by syndepositional processes. This mode of origin is at odds with the tectonic model (Earhart, 1988) that explains the metachert unit as a series of megablocks that slid into the trench filled by mafic volcanic rocks. More work is needed to clarify the structure and geochemistry of the metachert-basaltic metatuff contacts to resolve this problem. Earhart (1988) believed that the gold was in the cherty rocks when they slid off the continental shelf to the east. This may be correct, but there are structural and geochemical arguments that the Vandalia gold did not form in this manner. The facts that basaltic metatuff located a few meters to 100 m from gold-bearing metachert contains gold and that the geochemical signature of deposits in metachert and basaltic metatuff, as well as the Big Canyon-type deposits, are the same, lead me to favor formation at the same time. According to this concept, gold and associated elements (Na, As, and so forth) were introduced into the metachert following its metamorphism; the metachert was in contact with basaltic metatuff, regardless of whether the metachert is autochthonous or allochthonous. The gold is localized by ferrugenous layers in the metachert sequence, chiefly those with pyrite, which explains the apparent stratiform character of the Vandalia gold. The stratiform appearance of Vandalia gold also would be enhanced if fractures associated with faulting and folding occurred along bedding planes in metachert and between the metachert (a rigid block) and basaltic metatuff. Much of the Vandalia gold is in metachert immediately adjacent to basaltic metatuff, and some gold is in basaltic metatuff just below metachert, a geometry that is possibly explained by fracturing in rocks of different competence across the contact.

A chief ore control in this concept of epigenetic, postmetamorphic ore formation is the location of favorable pyritic beds in the metachert sequence. The pyritic beds are assumed to be synsedimentary because other iron minerals in the metachert formed with the chemical sediment, and there is no evidence for replacement of sedimentary iron oxides by sulfides. The lateral extent of potential Vandalia-type gold deposits is restricted to the occurrence of pyritic metachert. One goal of exploration is to define pyritic or formerly pyritic zones of metachert, some of which could lack surface exposure.

Comparison With Other Gold Deposits

The Vandalia deposit seems to be unusual in the Sierra Nevada foothills, chiefly because the metachert sequence is rare in this region. Although Logan (1938, p.

254) expressed the opinion that Vandalia is similar to other gold deposits in El Dorado County that occur in silicified and pyritized amphibolite, he did not recognize the pyritic metachert and BIF at Vandalia. Pyritic metachert and BIF are not well described in the literature for the foothills but may be present south of the Cosumnes River in the Melange Belt as described by Duffield and Sharp (1975). Regional mapping by Gold Fields Mining Corp. geologists traced occurrences of metachert and BIF, similar to that at Vandalia, for about 25 km from the Cosumnes River to the South Fork of the American River (M. Osterberg, written commun., 1987). Similar exhalative rocks may occur in other parts of the western foothills in volcanogenic settings that have produced Cu-Zn deposits that are now considered to be massive sulfide deposits (Albers, 1981). Some of the massive sulfide deposits contain significant amounts of gold, but these are polymetallic sulfide deposits that are geochemically different from the Vandalia deposit.

The Vandalia deposit may be analogous to some gold deposits in Archean exhalite and BIF; this is a common association (Boyle, 1979), but there is heated debate as to whether the gold was deposited with the sediments or was introduced later. Some workers hold that the gold is synsedimentary with the enclosing exhalative rocks (Hutchinson and others, 1971; Fripp, 1976), but others argue that the gold was introduced at a later time (for example, Phillips and others, 1984). The pendulum of opinion swings regarding syngenesis and epigenesis of gold in exhalite host rocks, but several empirical associations (Ridler, 1971; Hodgson and Mac-Geehan, 1982; and others) for the Archean deposits may also apply to deposits in El Dorado County: (1) One variety of gold deposit tends to be "gold-only"; (2) the exhalites occur in volcanic settings, commonly at the top of a mafic volcanic sequence, and some exhibit lateral facies changes into volcanic rocks (neither of which can be established at Vandalia); (3) many deposits are associated with intrusions (not known at Vandalia); and (4) many deposits are spatially associated with major faults that juxtapose mafic volcanic and sedimentary-exhalative rocks. The debate over the timing and significance of these associations is well illustrated by diverse opinions on the genesis of the recently discovered world-class gold deposits at Hemlo, Ontario.

The Vandalia deposit has some similarities to the Hemlo deposits that might reflect similar geochemical processes despite the many differences. The Hemlo deposits (Cameron and Hattori, 1985; Patterson, 1986) occur at the top of a mafic volcanic section at a facies change to clastic rocks. Parts of these magnetite-rich clastic rocks may have similarities to BIF's. The gold zones are in siliceous, highly potassic (sericitic) rocks that are rich in barite and molybdenite and contain abundant As, Sb, Hg, Tl, and V. Metamorphism to kyanite grade obscures textural relations in the ore zone. The abundant Hg, As, Sb, and Tl and siliceous character have led some observers to propose a hot spring or epithermal genesis (Patterson, 1986), but others, who are impressed by the deformation and widespread structurally controlled potassic alteration of the deposits, disagree with this hypothesis (Walford and others, 1986). The Vandalia deposits lack the extreme enrichment of Mo, Sb, and Hg and the unusual abundance of barite found at Hemlo, as well as its size and grade, but the moderate enrichment in volatile elements and Na (rather than K) may have generally similar implications for chemistry of fluids and structural controls.

Exploration Significance

The pyritic siliceous exhalite and associated lean BIF are distinctive rocks that should be good guides in exploration, especially because they are relatively well exposed in this area. Exploration can utilize either or both of two hypotheses: (1) Gold is syngenetic with the pyritic metachert, and (or) (2) gold is epigenetic and introduced along fractures and localized by the pyrite. If gold is indeed syngenetic, which I do not favor, there is evidence that gold is more abundant near post-metamorphic structures, thus structures seem to be important whether they acted to introduce or redistribute gold. Pyritic metachert units comparable in thickness to that at the Vandalia mine do not appear to be described in the literature, and if they are indeed rare or very thin in other parts of the foothills, then the potential for other Vandalia-type deposits would be low.

Geochemical Processes

Geochemical processes in the formation of Big Canyon- and Vandalia-type gold deposits seem to be generally similar despite differences in structure and host rock compositions. Both types of deposit exhibit enrichments in the same suite of elements (Na, P, S, CO_2, As, Sb, and REE) but negligible amounts of base metals, and in both types of deposits gold deposition favored rocks rich in iron. The PCA alteration and associated geochemical suite, which differs from that in most base-metal deposits, is a distinctive feature of "gold-only" ores in many parts of the world (for example, Boyle, 1979; Hodgson and MacGeehan, 1982; Kerrich, 1983). There probably are systematic differences in the origin and composition of the fluids responsible for transport and deposition of gold and associated metals relative to the fluids that produce base-metal deposits.

Alteration mineralogy in these "gold-only" deposits is distinctive and testifies to the character of the ore fluids. The alteration assemblage carbonate-albite-

pyrite ± chlorite ± muscovite is unusual for ore deposits (Meyer and Hemley, 1967), yet it is consistently associated with gold deposits in metamorphosed mafic rocks around the world, including world-class deposits of the Yellowknife district, Canada (Boyle, 1979), Kalgoorlie, Australia (Phillips, 1986), and the Abitibi greenstone belt of eastern Canada (Fryer and others, 1979; Kerrich, 1983; Robert and Brown, 1986). Although not much emphasized in the literature, many of these deposits show enrichment of phosphorous as apatite with gold. The chemistry and mineralogy of Na and K appear to be variable within this group of deposits—some deposits are characterized by Na loss and K enrichment in the form of muscovite, as emphasized by Kerrich (1983), whereas in other places such as Big Canyon, muscovite is minor but Na is fixed as abundant albite. This carbonate alteration reflects alkaline conditions with silicate mineralogy determined by ratios such as K/H^+, Na/H^+, and Na/K (Meyer and Hemley, 1967).

Fluid geochemistry can be elucidated by studies of fluid inclusions and stable isotopes. Fluid-inclusion and stable-isotopic studies of samples from the Mother Lode suggest temperatures of about 200–350 °C, pressures of about 0.6–2.5 kilobars, and the presence of CO_2-rich fluids (Coveney, 1981; Rosenbaum and Taylor, 1984; Weir and Kerrick, 1984; Bohlke and Kistler, 1986). Stable isotopic ratios from Mother Lode vein and alteration minerals suggest a deep crustal origin from metamorphic rocks. Fluid inclusions from Canadian and Australian gold deposits in metamorphic rocks suggest depositional temperatures of 300–500 °C, about 5 to more than 50 percent CO_2, the presence of methane in some inclusions, salinities generally less than seawater (3.6 weight percent NaCl), and pressures of about 1–3 kilobars (Kerrich, 1983; Phillips and Groves, 1983). Analyses of oxygen isotopes reveal enrichment in ^{18}O (Kerrich, 1983). This research has determined heavy oxygen isotopic ratios, high CO_2 contents, and presence of methane, which suggest the gold ore fluid is metamorphic in character. The ages determined for Mother Lode samples are not consistent with derivation during peak regional metamorphism as proposed by Kerrich and others but are consistent with deep crustal magmatism or metamorphism associated with subduction (Bohlke and Kistler, 1986).

There has been considerable discussion and speculation on the reasons for the unusual "gold-only" geochemical associations and apparent nontransport of Cu-Pb-Zn (reviewed by Kerrich, 1983; Phillips and Groves, 1983). Integration of data for mineral equilibria and fluid inclusions from gold deposits and results of experimental studies of ore solubilities suggest that if the ore fluids were about 300–500 °C, CO_2-rich, reducing, and alkaline, the most likely mechanism for gold transport would be by bisulfide complexes (Seward,

1984; Phillips and Groves, 1983). The practical application of this transport theory is that it predicts gold deposition in response to loss of aqueous sulfide, such as in the formation of pyrite or boiling; gold can also be precipitated from thio-complexes by oxidation and decrease in pH from alkaline to neutral. The mechanism of gold deposition in the Vandalia-type deposit is less clear than for the Big Canyon-type deposit if gold is indeed superimposed on earlier pyrite at Vandalia. However, the amount of feldspar and mica in the pyritic metachert might be too small to buffer pH in that rock; if the pH in the chert was lower than in enclosing rocks, this might have been sufficient to cause gold deposition.

CONCLUSIONS

Gold deposits in the Big Canyon area probably are related in time and process despite their differences in host rocks and local structure. The Big Canyon and Live Oak deposits are clearly related to post-Jurassic, post-metamorphic structures that splay from the Big Canyon fault, which is a major discontinuity between contrasting terranes. The Big Canyon-type deposits are in highly fractured zones with numerous veins that result in wide zones (10–30 m) of PCA rock that carries gold in the range of about 1–10 g/t, as well as in locally richer streaks. The gold zones are a combination of veinlet filling and replacement of basaltic metatuff and metadiorite. The gold zones are enriched in Na, Ca, P, S, CO_2, and rare elements (As, Sb, Se, Te, and REE), but base metals (Cu, Pb, and Zn) and Ag are not notably enriched. Formation of the alteration and ore minerals is consistent with alkaline, CO_2-rich, hydrothermal (about 300–400 °C) fluids of metamorphic origin as determined for Mother Lode deposits and other similar gold deposits.

The Vandalia deposit occurs chiefly in pyritic metachert, which is part of a sequence that formed as a chemical sediment (volcanogenic exhalite). Gold favors strata rich in pyrite; the pyrite is probably synsedimentary, but the gold probably is epigenetic. The richest gold values are in fractured zones in which pyrite is largely on fractures, and the metachert contains more than 1 percent Na as albite and several percent carbonate. The gold-rich samples from the Vandalia deposit contain elevated concentrations of the same major- and minor-element suites as found in the Big Canyon-type deposits. Although the timing and details of structures in the Vandalia deposit are not well understood, it is possible that second-order fractures related to the Big Canyon fault broke the metamorphic rocks at Vandalia at boundaries of metachert and balsaltic metatuff units and along bedding and allowed inflow of hydrothermal fluids similar to those that formed the Big Canyon deposit. By

this concept of postmetamorphic mineralization, gold was localized by reactions with iron minerals in zones of brittle fractures.

The Big Canyon-type deposits display structural controls and alteration that are similar to deposits of the Mother Lode and other "gold-only" deposits in metamorphic rocks around the world which account for a major part of world gold production and many world-class deposits. The suture between the Mother Lode belt and the melange belt, which is locally the Big Canyon fault, and especially second-order faults related to that zone of deformation are favorable sites for development of these deposits. Useful guides to gold along these structures include PCA alteration and enrichment in rare elements. Iron-rich rocks are most favorable for reactions that localize gold. Pyritic and hematitic strata in siliceous exhalite were favored at the Vandalia deposit, but similar rocks do not seem to be present in significant amounts elsewhere in the Sierra Nevada foothills, thus the potential for other deposits similar to the Vandalia seems low. The known zones of major faults that cut mafic rocks outline large areas in the Sierra Nevada foothills that are highly favorable for the occurrence of Big Canyon-type deposits

REFERENCES CITED

Albers, J.P., 1981, A lithologic-tectonic framework for the metallogenic provinces of California: Economic Geology, v. 76, p. 765–790.

Bohlke, J.K., and Kistler, R.W., 1986, Rb-Sr, K–Ar, and stable isotope evidence for the ages and sources of fluid components of gold-bearing quartz veins in the northern Sierra Nevada Foothills metamorphic belt: Economic Geology, v. 81, p. 296–322.

Boyle, R.W., 1979, The geochemistry of gold and its deposits: Geological Survey of Canada Bulletin 280, 584 p.

Cameron, E.M., and Hattori, Keiko, 1985, The Hemlo gold deposit, Ontario—a geochemical and isotopic study: Geochimica et Cosmochimica Acta, v. 49, p. 2041–2050.

Clark, L.D., 1964, Stratigraphy and structure in part of the western Sierra Nevada metamorphic belt, California: U.S. Geological Survey Professional Paper 410, 70 p.

———— 1976, Stratigraphy of the north half of the western Sierra Nevada metamorphic belt, California: U.S. Geological Survey Professional Paper 923, 26 p.

Clark, W.B., and Carlson, D.W., 1956, Mines and mineral resources of El Dorado County, California: California Journal of Mines and Geology, v. 52, p. 369–591.

Coveney, R.M., Jr., 1981, Gold quartz veins and auriferous granite at the Oriental mine, Allegheny district, California: Economic Geology, v. 70, p. 2176–2199.

Crock, J.G., Lichte, F.E., and Briggs, P.H., 1983, Determination of elements in NBS geological reference materials SRM 278 obsidian and SRM 688 basalt by ICAP–AES: Geostandards Newsletter, v. 7, no. 2, p. 335–340.

Davis, J.C., 1986, Statistics and data analysis in geology (2d ed.): New York, John Wiley, 646 p.

Duffield, W.A., and Sharp, R.V., 1975, Geology of the Sierra Foothills melange and adjacent areas, Amador County, California: U.S. Geological Survey Professional Paper 827, 30 p.

Earhart, R.L., 1988, Geologic setting of gold occurrences in the Big Canyon area, El Dorado County, California: U.S. Geological Survey Bulletin 1576, 13 p.

Ferguson, H.G., and Gannett, R.W., 1932, Gold-quartz veins of the Allegheny district, California: U.S. Geological Survey Professional Paper 172, 139 p.

Fripp, R.E.P., 1976, Stratabound gold deposits in Archean banded iron-formation, Rhodesia: Economic Geology, v. 71, p. 58–75.

Fryer, B.J., Kerrich, R., Hutchinson, R.W., Peirce, M.G., and Rogers, D.S., 1979, Archean precious metals hydrothermal systems, Dome mine, Abitibi greenstone belt, Part I: Canadian Journal of Earth Sciences, v. 16, p. 421–439.

Gross, G.A., 1980, A classification of iron formations based on depositional environments: Canadian Mineralogist, v. 18, p. 215–222.

Hodgson, C.J., and MacGeehan, P.J., 1982, A review of the geological characteristics of "gold-only" deposits in the Superior Province of the Canadian Shield, in Hodder, R.W., and Petruk, W., eds., Geology of Canadian gold deposits: Canadian Institute of Mining and Metallurgy Special Volume 24, p. 211–232.

Hubert, A.E., and Chao, T.T., 1985, Determination of gold, indium, tellurium, and thallium in the same sample digestion of geological materials by atomic absorption spectroscopy and two-step solvent extraction: Talanta, v. 32, p. 568–570.

Hutchinson, R.W., Ridler, R.H., and Suffel, G.G., 1971, Metallogenic relationships in the Abitibi Belt, Canada—a model for Archean metallogeny: Canadian Institution of Mining and Metallurgy Transactions, v. 74, p. 106–115.

Jackson, L.L., Brown, F.W., and Neil, S.T., 1988, Major and minor elements requiring individual determinations, classical whole rock analysis, and rapid rock analysis, in Baedecker, P.A., ed., Methods for geochemical analysis: U.S. Geological Survey Bulletin 1770–G, p. G1–G23.

James, H.L., 1954, Sedimentary facies of iron-formation: Economic Geology, v. 49, p. 235–293.

Kerrich, R.W., 1983, Geochemistry of gold deposits in the Abitibi greenstone belt: Canadian Institute of Mining and Metallurgy Special Volume 27, 75 p.

Knopf, Adolf, 1929, The Mother lode system of California: U.S. Geological Survey Professional Paper 157, 88 p.

Landefeld, L.A., Silberman, M.L., and O'Leary, R.M., 1986, Geology and geochemistry of the Mother Lode gold belt, California, compared with Archean lode gold deposits: Geological Society of South Africa, Extended Abstracts of Geocongress '86, p. 311–314.

Le Maitre, R.W., 1976, The chemical variability of some common igneous rocks: Journal of Petrology, v. 17, p. 589–637.

Logan, C.A., 1938, Mineral Resources of El Dorado County: California State Division of Mines, California Journal of Mines and Geology, v. 34, p. 206–280.

Loyd, R.C., Anderson, T.P., and Bushnell, M.M., 1983, Mineral Land classification of the Placerville 15' quadrangle, El Dorado and Amador Counties, California: California Division of Mines and Geology Open-File Report 83–29 SAC, 45 p.

Meyer, Charles, and Hemley, J.J., 1967, Wall rock alteration, *in* Barnes, H.L., ed., Geochemistry of hydrothermal ore deposits: New York, Holt, Rinehart, and Winston, p. 166–235.

Osterberg, Mark, 1984, Generalized geologic map of the Big Canyon project area, El Dorado County, California: Gold Fields Mining Co., field trip map, scale 1:12,000.

Osterberg, Mark, Willis, Jerry, and Zimmerman, John, 1984, Geologic map and drill logs, Big Canyon project, El Dorado County, California: Gold Fields Mining Co., unpublished reports.

Patterson, G.C., 1986, Regional field guide to the Hemlo area: Geological Association of Canada, Field Trip 4 Guidebook, The Hemlo Gold Deposits, Ontario, p. 1–27.

Phillips, G.N., 1986, Geology and alteration in the Golden Mile, Kalgoorlie: Economic Geology, v. 81, p. 779–808.

Phillips, G.N., and Groves, D.I., 1983, The nature of Archean gold-bearing fluids as deduced from gold deposits of Western Australia: Geological Society of Australia Journal, v. 30, p. 25–39.

Phillips, G.N., Groves, D.I., and Martyn, J.E., 1984, An epigenetic origin for Archean banded iron-formation-hosted gold deposits: Economic Geology, v. 79, p. 162–171.

Ridler, R.H., 1971, Relationship of mineralization to stratigraphy in the Archean Rankin Inlet-Ennadai belt: Canadian Mining Journal, v. 92, no. 2, p. 50–53.

Robert, Francois, and Brown, A.C., 1986, Archean gold-bearing quartz veins at the Sigma Mine, Abitibi greenstone belt, Quebec—Part II, Vein paragenesis and hydrothermal alteration: Economic Geology, v. 81, p. 578–616.

Rosenbaum, Steve, and Taylor, B.E., 1984, Sources and temperatures of ore fluids in the northern Mother Lode, California (Allegheny district)—oxygen and carbon isotope evidence: Geological Society of America Abstracts with Programs, v. 16, p. 639.

Saleeby, J.B., 1982, Polygenetic ophiolite belt of the California Sierra Nevada—geological and tectonostratigraphic development: Journal of Geophysical Research, v. 87, no. B3, p. 1803–1824.

Schuiling, R.D., and Vink, B.W., 1967, Stability relations of some titanium-minerals (sphene, perovskite, rutile, anatase): Geochimica et Cosmochimica Acta, v. 31, p. 2399–2411.

Seward. T.M., 1984, The transport and deposition of gold in hydrothermal systems, *in* Foster, R.P., ed., Gold '82—the geology, geochemistry, and genesis of gold deposits: Rotterdam, A.A. Balkema, for the Geological Society of Zimbabwe, Special Publication No. 1, p. 165–181.

Springer, R.K., 1980, Geology of the Pine Hill intrusive complex, a layered gabbroic body in the western Sierra Nevada foothills, California, Part 2: Geological Society of America Bulletin, v. 91, p. 1536–1626.

Taggart, J.E., Jr., Lindsay, J.R., Scott, B.A., Vivit, D.V., Bartel, A.J., and Stewart, K.C., 1988, Analysis of geologic materials by wave-length-dispersive X-ray fluorescence spectrometry, *in* Baedecker, P.A., ed., Methods for geochemical analysis: U.S. Geological Survey Bulletin 1770–E, p. E1–E19.

Wagner, D.L., Jennings, C.W., Bedrossian, T.L., and Bortugno, E.J., 1981, Geologic map of the Sacramento quadrangle: California Division of Mines and Geology Regional Geologic Map 1A, scale 1:250,000.

Walford, P.C., Weiker, R., and Guthrie, R., 1986, The Page-Williams property: Geological Association of Canada, Field Trip 4 Guidebook, The Hemlo Gold Deposits, Ontario, p. 53–61.

Weir, R.H., and Kerrick, D.M., 1984, Mineralogic and isotopic relationships in gold-quartz veins in the southern Mother Lode, California: Geological Society of America Abstracts with Programs, v. 16., p. 688.

Wells, J.D., and Mullens, T.E., 1973, Gold-bearing arsenian pyrite determined by microprobe analysis, Cortez and Carlin gold mines, Nevada: Economic Geology, v. 68, p. 187–201.

Wilson, S.A., Kane, J.S., Crock, J.G., and Hatfield, D.B., 1988, Chemical methods of separation for optical emission, atomic absorption, spectrometry, and colorimetry, *in* Baedecker, P.A., ed., Methods for geochemical analysis: U.S. Geological Survey Bulletin 1770–D, p. D1–D14.

DESCRIPTION OF CHEMICALLY ANALYZED

ROCK SAMPLES

and

METHODS AND RESULTS OF GEOCHEMICAL ANALYSES

APPENDIX I. DESCRIPTION OF CHEMICALLY ANALYZED ROCK SAMPLES

[All samples are from drill core; drill sites are shown on figure 2. Sample numbers relate to drill-hole nomenclature—for example, BC2-135: BC = Big Canyon project (LO = Live Oak prospect); 2 = hole 2; 135 = depth 135 ft. Two types of information are given: M, macroscopic features; P, petrographic features observed in thin sections in transmitted and reflected light]

Definitions: "carbonate" is nonspecific for calcite, ankerite, dolomite, and so forth, but where calcite is stated that is specific for the mineral that reacts strongly to dilute hydrochloric acid. Grade (generalized from gold assays): high, > 0.1 oz/t; medium, 0.02–0.1 oz/t; low, 0.005–0.2 oz/t; barren, Au not detected (< 0.005 oz/t); material sampled and analyzed by U.S. Geological Survey may not be the same as analyzed by Gold Fields Mining Corp.

BC2-135. M: gray micaceous metachert with 2 percent pyrite; medium grade. P: mostly microgranular quartz (75 μm) with 20 percent intergrown carbonate rhombs and veinlets; 5 percent fine hematite; 2 percent pyrite (20–300 μm); trace chlorite.

BC2-147. M: gray micaceous metachert; sparse pyrite; low grade.

BC2-169. M: tan and gray partly weathered dike with massive fabric and porphyritic texture; barren. P: porphyritic texture of plagioclase phenocrysts set in microgranular matrix of plagioclase plus Fe-Mg silicates that are altered to chlorite. This is probably an altered diabase dike.

BC2-212. M: light-gray thinly laminated micaceous metachert with traces of pyrite on beds; barren.

BC2-322. M: gray fractured and veined metachert; abundant (10 percent) pyrite on beds and in veinlets; high grade.

BC4-92. M: tan metachert; originally 5 percent pyrite, most of which is oxidized to limonite; iron oxides in joints; low grade.

BC4-103. M: white to cream-colored metachert; 1 percent pyrite that is partly oxidized; barren.

BC4-605. M: green-gray laminated basaltic metatuff; swirled beds; weakly altered; scattered calcite veinlets; low grade. P: millimeter-scale layers of leucocratic (quartz plus albite) and layers of mafic minerals (chlorite plus epidote); disseminated carbonate and veinlets of carbonate.

BC4-630. M: tan siliceous pyrite-carbonate-altered rock, probably basaltic metatuff; 8 percent pyrite; disseminated carbonate and veinlets of carbonate; low grade. P: original textured wiped out; granular PCA rock with no Fe-Mg silicates; swaths of coarse albite and carbonate as wide as 400 μm; abundant coarse sphene with rutile overgrowths; 2 percent apatite in albite.

BC4-656. M: tan silica-pyrite-carbonate alteration of basaltic metatuff; 20 percent pyrite in veinlets; medium grade. P: microgranular quartz-albite rock with no Fe-Mg silicates; veinlets of quartz, albite, carbonate, pyrite, and minor chlorite; disseminated apatite, sphene, and rutile.

BC4-669. M: tan calcite-silica-pyrite-altered basaltic metatuff; traces of galena; medium grade. P: granular albite-carbonate rock with variable fine to coarse grains and no Fe-Mg silicates; albite and carbonate tend to be in separate swaths; minor late chlorite in veinlets with carbonate; 1 percent microgranular disseminated sphene.

BC4-683. M: gray pervasively silicified and pyritized basaltic metatuff breccia; medium grade.

BC4-701. M: tan pervasively PCA altered, basaltic metatuff; 10 percent pyrite; high grade. P: swirled swaths of granular albite and carbonate with abundant disseminated pyrite and microgranular sphene; only Fe-Mg silicate is minor late chlorite; several 3–30-μm gold grains.

BC4-773. M: gray granular alteration zone; looks almost like unbedded quartzite; disseminated pyrite and carbonate; late calcite veinlets; high grade; protolith basaltic metatuff? P: coarse granular albite-carbonate rock; early albite with pyrite is cut and replaced by carbonate; 5 percent late pale-green chlorite is only Fe-Mg silicate; disseminated sphene and rutile in albite; one 4 μm gold grain.

BC4-781. M: slightly altered basaltic metatuff at lower boundary of gold zone; mostly green laminated basaltic metatuff with some tan PCA alteration along veinlets; barren.

BC5-95. M: tan and gray oxidized pyrite metachert with dark Fe-silicate layers; originally 5 percent pyrite, some pyrite is fresh; medium grade

BC5-98. M: dark-gray hematitic metachert (lean BIF); some pyrite on beds; low grade.

BC7-25. M: brown highly oxidized, laminated metachert rich in hematite and earthy iron oxides; probably had 10 percent pyrite to make iron oxides; medium grade.

BC7-55. M: gray highly pyritic (20 percent) metachert; some pyrite in veinlets, most pyrite is fresh; this gold zone is more fractured and pyritic than adjacent metachert; high grade. High iron content caused interference problems in XRF analysis.

BC8-84. M: ocher oxidized, laminated metachert; limonite after pyrite along beds and in joints; barren.

BC8-135. M: gray laminated metachert; only slightly oxidized; dark layers of hematite; barren.

BC8-218. M: zone of fractured and weathered metachert; soft ocher clay is abundant; medium grade.

BC8-252. M: white and tan metachert with 1-cm-thick layers and veinlets filled with pyrite and earthy iron oxides; appears to be supergene altered fracture zone; medium grade.

BC8-499. M: tan laminated basaltic metatuff with pyrite-carbonate alteration; 3 percent pyrite; barren.

BC8-501. M: tan pyrite-carbonate-altered basaltic metatuff breccia; early breccia is overprinted by alteration; 5 percent pyrite in veinlets and disseminated; barren.

BC9-210. M: gray metachert with micaceous layers; trace hematite; barren.

BC9-225. M: pale-gray dike; aphanitic texture; one of several massive rocks that crosscut the metachert sequence in this interval; I picked the hardest, least altered 1-ft interval; barren. P: porphyritic rock with plagioclase phenocrysts in aphanitic matrix.

BC9-243. M: dark-gray laminated metachert with hematitic layers; 5 percent hematite overall?; nonmagnetic; low grade.

BC9-348. M: dark-green laminated basaltic metatuff; more than 100 ft thick like this—composition uniform overall, millimeter-scale felsic and mafic layers; not foliated; barren.

BC10-63. M: gray chert with 3 percent pyrite; medium grade. P: microgranular texture of intergrown silicates which are mostly albite; some albite has radial texture; only Fe-Mg silicate is late pale-green chlorite; no carbonate; coarse pyrite randomly disseminated, not layered; abundant needles of honey-colored

rutile; 1 percent disseminated apatite and trace hematite. Highly altered basaltic metatuff?

BC10–74. M: gray bedded pyritic metachert; sample chosen for high pyritic content that seems to be on beds; medium grade. P: layers shown by variations in grain size and by pyrite and riebeckite; swaths of albite and carbonate are coarser than microgranular quartz and have apatite; tiny (5 μm) inclusions of high-index silicate in quartz may be epidote; disseminated tiny hematite intergrown with quartz; no sphene or rutile seen. Odd rock! PCA-altered metachert?

BC10–101. M: green thinly laminated, basaltic metatuff; 2 percent pyrite; barren. P: layers composed of quartz-albite and of chlorite-epidote; abundant chlorite (30 percent); 5 percent hematite; scattered trace pyrite; 4 percent sphene.

BC10–111. M: gray and tan finely laminated hematite-pyrite metachert; medium grade. P: chiefly microcrystalline quartz; scattered rhombs and veinless carbonate; abundant lathes of hematite (20 percent in gray layers); iron oxides in place of cubic pyrite; trace sphene; one flake of 3-μm gold.

BC10–127. M: gray thinly laminated metachert; slump folds locally tight; low grade. P: chiefly microcrystalline quartz; 5 percent micas (chlorite and muscovite) oriented along beds; rare opaques; trace sphene; no albite recognized.

BC11–48. M: tan laminated lean iron metachert; weathered, argillized?; medium grade. P: >90 percent microcrystalline quartz; 5 percent clay; sprays of fine riebeckite; oxidized pyrite.

BC11–145. M: tan, finely laminated limonitic (ex-pyrite) metachert; iron oxides in fractures; low grade. P: Chiefly microcrystalline quartz; scattered 2 percent pyrite altered to iron oxides.

BC11–213. M: gray faintly laminated lean iron metachert; no oxidation; barren.

BC16–46. M: tan weathered metachert; limonite in fractures; high grade.

BC16–101. M: tan altered basaltic metatuff; layered; pyritic; veinlets of carbonate; low grade. P: thin layers marked by opaque minerals and rutile; abundant albite; needles of blue pleochroic sodic actinolite; golden rutile (4 percent); pocky coarse pyrite; several specks of gold. PCA-altered mafic rock, possibly a dike.

BC24–82. M: dark-gray pyritic argillite; bleached a bit in this area near fault and adjacent PCA alteration below 88 ft; barren. Note high Na in chemical analysis.

BC24–94. M: tan breccia, PCA-altered metadiorite?; veinlets of pyrite and carbonate; medium grade. P: gash veins filled by coarse pyrite and carbonate cut very fine microcrystalline rock composed chiefly of untwinned albite and fine carbonate with fine hematite; greener, less altered parts have chlorite. Protolith might have been argillite rather than metadiorite, but original texture is obscure.

BC24–120. M: tan and gray altered and brecciated aphanitic rock, metadiorite? Pyritic with late calcite veinlets; low grade. P: microgranular quartz and albite (can not tell abundances because albite not twinned); rare mafic silicates; disseminated pyrite and sphene; coarse calcite veinlets.

BC27–182. M: tan pyritic breccia; many late calcite veinlets; breccia was prealteration because fragments alter differently; medium grade. P: relicts of actinolitic magnetite texture largely wiped out by albite flooding; microgranular albite grades to coarser carbonate-albite rock with disseminated pyrite, cut by coarse calcite veinlets; rutile (elongate, striated crystals, honey colored in transmitted light) abundant as 100 μm crystals in PCA-altered rock.

BC27–204. M: green slightly altered basaltic metatuff breccia with sparse disseminated and vein calcite; low grade. P: fragmental texture; some clasts are layered; chiefly albite plus carbonate; disseminated hematite, pyrite, and rutile; late veinlets of carbonate and chlorite.

BC29–168. M: tan pyritic metadiorite breccia; gray slightly altered metadiorite at 155 ft; stope of Big Canyon mine hit at 193 ft; high grade. P: albite-carbonate microgranular rock; replaced earlier breccia. Earliest albite is microgranular with little carbonate; cut by veinlets of coarse-grained-chlorite-pyrite-minor albite; later cut by veinlets of coarse carbonate-albite-pyrite; microgranular sphene has boxwork texture.

BC29–171. M: tan pyritic metadiorite breccia; high grade. P: microgranular albite rock cut by carbonate veinlets; early albite has elongate feathery morphology; grades to coarser twinned tabular crystals; apatite and sphene in albite; 6 percent disseminated pyrite.

BC31–433. M: green slightly altered metadiorite breccia with only a few calcite veinlets; barren.

BC31–436. M: tan and green moderately altered metadiorite breccia with about 10 percent pyrite and many calcite veinlets; high grade. P: centimeter-sized fragments replaced by intergrown albite with fine chlorite; cut by coarse carbonate veinlets with chlorite; abundant pyrite in albite and in carbonate veinlets.

BC31–476. M: tan and gray pyritic basaltic metatuff; layered or sheared; high grade. P: shear foliation defined by aligned crystals of albite and actinolite; albite-actinolite-chlorite-pyrite-carbonate rock cut by late coarse calcite veinlets; disseminated microgranular sphene.

BC31–485. M: gray aphanitic rock; diffuse alteration; calcite veinlets have no selvages; high grade. P: original texture destroyed by albite flooding; no Fe-Mg silicates present; microgranular albite cut by quartz veinlets and carbonate veinlets; disseminated apatite and sphene in albite; a few flakes of 2-μm gold.

BC31–498. M: gray metadiorite; slightly altered, but a few quartz(?) and pyrite veinlets; low grade. P: microgranular albite abundant with 10 percent interstitial fine chlorite, traces of sericite, and scattered rhombs of carbonate; cut by quartz-albite-pyrite veinlets; disseminated pyrite (5 percent) and microgranular sphene.

BC32–339. M: tan stockwork veined and brecciated basaltic metatuff; alteration pervasive here in gold zone; medium grade. P: abundant fine and coarse albite and carbonate; prismatic actinolite (5 percent); later chlorite and sericite (5 percent); coarse disseminated pyrite (7 percent); disseminated coarse sphene and trace of fine needles of rutile; a few flakes of 2–3-μm gold.

BC32–356. M: green slightly altered basaltic metatuff; minor disseminated carbonate; medium grade. P: textures of tuff layers survive; some layers are 50 percent pale-green chlorite; abundant albite in light layers; cut by albite-carbonate veinlets; disseminated apatite in albite, 3 percent pyrite, rutile, and microgranular sphene; several specks of 2-μm gold.

BC32–373. M: tan altered basaltic metatuff; 3 percent pyrite; low grade. P: weakly layered rock with 30 percent albite, 25

percent carbonate, 20 percent chlorite, 10 percent actinolite, plus fine disseminated epidote (2 percent) and pyrite (5 percent); cut by carbonate veinlets with no alteration selvage; disseminated microgranular sphene that forms aggregates; several 2–5-μm gold flakes.

BC32–393. M: green slightly altered basaltic metatuff; disseminated carbonate and about 2 percent pyrite; barren. P: thin layers of albite plus actinolite veinlets. Chlorite; cut by swaths of carbonate that replace(?) chlorite; fine hematite in chlorite; disseminated microgranular sphene and euhedral pyrite.

BC32–672. M: light-gray metachert with faint layers marked by 1 percent pyrite and cut by thin pyrite veinlets; barren. P: chiefly microgranular quartz of 20–200-μm size; scattered fine rhombs of carbonate (5 percent); albite (5 percent, some twinned); chlorite plus actinolite (5 percent) intergrown with quartz; disseminated euhedral pyrite (2 percent); trace hematite; rare microgranular sphene.

BC32–705. M: medium-gray metachert with 5 percent pyrite that defines swirled beds; medium grade. P: chiefly microgranular quartz with swaths or layers of albite (10 percent), carbonate (5 percent), and chlorite plus actinolite (10 percent); disseminated lathes of hematite (2 percent), pyrite (4 percent), and microgranular sphene (3 percent); a few grains of gold(?).

BC32–718. M: medium-gray pyritic metachert with fine layers of dark minerals; medium grade. P: fine layers suggested by differences in quartz grain size and thin layers of fine actinolite or pyrite; swaths of carbonate (5 percent) and albite (10 percent); disseminated fine hematite (1 percent) and sparse sphene; a few 2-μm grains of gold.

BC32–742. M: dark-reddish-gray hematitic metachert; barren. P: fine lamination shown by layers rich in pyrite, hematite, or fine Na-actinolite (riebeckite?); cut by late veinlets of carbonate (5 percent); seems to be mostly microgranular quartz; no twins in 30-μm grains to indicate albite as is likely by high Na content; abundant (20 percent) 5–20-μm hematite in some layers exceeds pyrite.

BC32–765. M: gray pyritic metachert; faint laminae of mafic silicates and pyrite are swirled; medium grade. P: layers marked by different quartz grain size and fine hematite, pyrite, or actinolite-epidote-sphene; some albite is shown by twins in coarser grains, but most is not evident; two flakes of gold.

BC32–776. M: green layered basaltic metatuff with scattered calcite veinlets and 1 percent pyrite; barren. P: vague layering produced by shear? Approximately equal amounts of albite, epidote, and actinolite, plus splotches of carbonate (10 percent); abundant microgranular sphene in 100-μm aggregates; sparse pyrite.

BC34–777. M: dark-green massive amphibolite or metadiorite; sparse carbonate and pyrite; barren.

BC34–794. M: similar to 777-ft sample; dark-green amphibolite; low carbonate and pyrite, 2 ft from Au-alteration zone; barren. P: granular texture of intergrown albite-actinolite-epidote in equal amounts; gash fractures filled by carbonate and albite; disseminated magnetite and microgranular sphene.

BC34–796. M: tan alteration zone 0.3 m wide centered on pyrite-carbonate veinlets; cuts amphibolite as at 777 ft; low grade. P: granular albite-actinolite rock, replaced by carbonate, chlorite, and pyrite (5 percent); abundant microgranular sphene; one 4-μm gold grain.

BC34–800. M: tan altered amphibolite; more pyrite and carbonate than at 796 ft; medium grade. P: granular intergrown albite, pale-green amphibole, and pyrite (10 percent); cut by veinlets of coarser albite and carbonate and late stringers of chlorite; abundant disseminated sphene, much intergrown with pyrite; one 2-μm speck of gold.

BC34–802. M: tan altered amphibolite; abundant carbonate but low pyrite; barren. P: vague mineral layering indicates shear?; rock is microgranular albite-chlorite-actinolite, cut by veinlets of coarse carbonate with chlorite selvage; disseminated cubic magnetite and pyrite; granular sphene.

LO4–116 Live Oak prospect. M: green mafic breccia (metadiorite?); sample chosen to be little altered for background; barren.

LO4–124. M: dark-gray amphibolite or metadiorite(?) breccia; 5 percent pyrite; medium grade. P: layers of albite (50 percent), carbonate (25 percent), and actinolite (20 percent); disseminated pyrite and 20-μm sphene.

LO4–157. M: dark-gray less altered amphibolite adjacent to 0.6 m of tan PCA alteration; barren.

LO5–42. M: tan pyritic metabasalt breccia; hardness suggests silicification; medium grade. P: PCA-altered rock in which early feathery albite grades to swaths of coarse albite and carbonate, cut by veinlets of coarse carbonate; disseminated pyrite (2 percent), sphene, and rutile in albite; one flake of gold.

LO5–46. M: tan siliceous-pyritic breccia, medium grade. P: albite of different grain sizes mimics breccia fragments; early albite is microgranular, later swaths of albite are coarser and twinned; erratic swaths of 10-μm and 100-μm pyrite; trails of 20-50-μm sphene; one flake of gold in pyrite.

LO5–125. M: dark-green metabasalt breccia adjacent to Au zone; 2 percent pyrite; scattered carbonate veinlets; barren.

LO7–59. M: tan pyritic metabasalt breccia; disseminated carbonate; this is a thin Au zone; low grade. P: abundant albite (microgranular to coarser with twins) intergrown with fine rhombs of coarse carbonate (30 percent); traces of fibrous amphibole bleached to pale green; abundant 20–40-μm pyrite; disseminated sphene and hematite; several grains 3-μm gold.

LO7–75. M: dark-green weakly altered metabasalt breccia; background sample; barren.

LO7–86. M: tan siliceous pyritic breccia; high grade. P: PCA-altered rock; traces of bleached fibrous amphibole. Grains of albite and carbonate variable 20–400 μm in size, coarse grains probably filled veins; scattered coarse pyrite, apatite, and microgranular sphene aggregates in albite with traces of fine hematite.

LO7–102. M: tan siliceous pyritic breccia; medium grade. P: original texture wiped out; microgranular albite cut by veinlets of coarse albite and carbonate; small amount of chlorite but no other Fe-Mg silicates; disseminated 20-μm sphene and 50-μm rutile needles and sparse pyrite; a few 2-μm gold grains.

LO7–109. M: tan siliceous pyritic breccia; medium grade. P: original texture gone; no Fe-Mg silicates; abundant albite— early feathery albite crystals grade to coarser ones with twinning in swaths with carbonate; 30-μm microgranular sphene, rutile, and hematite in albite; 3 percent pyrite is coarse (100–200 μm), one 3-μm gold grain.

LO7–125. M: dark-green-gray weakly altered metabasalt or metadiorite; barren. P: mineral layers produced by shear?

Overall, albite > sodic actinolite > carbonate; inclusions of 20-μm hematite, sphene, and epidote in albite.

LO7–142. M: light-gray siliceous breccia; twice fractured and cut by pyrite-carbonate veinlets; low grade. P: multiple veins cut fragments; rock is chiefly albite-carbonate-pyrite as replacement and vein filling; only outlines of fragments survive; abundant < 30-μm pyrite and hematite; streaks of microgranular sphene.

APPENDIX II. METHODS AND RESULTS OF GEOCHEMICAL ANALYSES

[Rock samples were analyzed by chemists of the U.S. Geological Survey using standard methods described below. For more information consult the references cited]

X-Ray Fluorescence (XRF): Sample (0.8 g) is fused in lithium tetraborate, and the glass disk is analyzed for major elements by wavelength-dispersive X-ray spectrometry (Taggart and others, 1988). Limits of detection shown in table 5. J.E. Taggart and A.J. Bartel, analysts.

Induction Coupled-Plasma Atomic Emission Spectroscopy (ICP): Sample (0.2 g) is digested with mixed acids (HF, HCl-HNO$_3$, HClO$_4$) to dryness, then redissolved in HCl-HNO$_3$, then analyzed by induction-coupled plasma atomic emission spectroscopy with lutetium as an internal standard (Crock and others, 1983); Lower limits of detection in table 5. A few refractory minerals are not dissolved by this acid attack; specifically, for B in tourmaline and Zr in zircon, the sample is fused in Na$_2$O$_2$ prior to ICP analysis for B and Zr. Paul Briggs, analyst.

Special Element Analysis: Six additional elements and H$_2$O and Co$_2$ were analyzed on request as shown below. L.L. Jackson, E.E. Engleman, D.B. Hatfield, and E. Brandt, analysts. Methods are described by Wilson and others (1988) and by Jackson and others (1988).

Fe as FeO: Sample (0.5 g) is decomposed with HF and H$_2$SO$_4$, and the digestate is treated with solution of H$_3$BO$_3$, H$_2$SO$_4$, and H$_3$PO$_4$. Fe(II) is determined by potentiometric titration.

H$_2$O: Sample (1.0 g) is heated at 110 °C for one hour, and H$_2$O$^-$ is determined by weight loss. H$_2$O$^+$ is determined on 0.05-g sample heated with lead oxide and lead chromate, and evolved water is analyzed by coulometric Karl Fischer titration.

CO$_2$: Sample (0.05 g) is decomposed in 2 M perchloric acid, and evolved CO$_2$ is determined as an acid by coulometric titration.

S$_{total}$: Sample (0.25 g) is mixed with vanadium pentoxide and combusted at 1370 °C in oxygenated atmosphere; S$_{total}$ is determined at SO$_2$ by infrared absorption spectroscopy.

Au: Sample (10 g) is digested with HBr-Br$_2$, and Au is extracted with methyl-isobutyl ketone. After washing the organic phase with 0.1 M HBr to remove iron, Au is determined by flame atomic absorption spectroscopy (Hubert and Chao, 1985).

Hg: Sample (0.1 g) is decomposed in closed vessel with HNO$_3$ and sodium dichromate, then Hg(II) is reduced by hydroxylamine hydrochloride-sodium chloride and stannous chloride; Hg vapor is transported to and measured in an absorption cell using atomic absorption spectroscopy.

Se: Sample (0.3 g) is digested with K$_2$S$_2$O$_8$, HF, HNO$_3$, and HClO$_4$ plus a second treatment by HNO$_3$ and HClO$_4$ plus H$_2$SO$_4$. Solution is mixed with sodium borohydride, and resultant metal hydride is carried in an argon stream into a heated quartz glass tube and determined by atomic absorption spectroscopy.

Te: Sample is treated as for Au analysis; Te is extracted into methyl-isobutyl ketone, HBr is added to remove iron, and Te is determined by flame atomic absorption spectroscopy.

Table 4. Analytical results for rock samples from the Big Canyon area

[N, not detected; II, not determined because of interference usually caused by high iron content; <, detected but below the limit of determination shown; >, determined to be greater than the value shown; S (as in Fe%-S), determined by ICP-AES. Type sample explained in footnote No. 2 at end of table]

Sample	SiO$_2$%	Al$_2$O$_3$%	[3]FeTO$_3$%	FeO%	MgO%	CaO%	Na$_2$O%	K$_2$O%	TiO$_2$%	P$_2$O$_5$%
BC10-101	49.1	17.20	13.50	7.90	4.90	4.03	5.07	0.61	2.42	0.32
BC10-111	56.2	2.04	13.00	.0H	3.19	7.27	1.07	.13	.38	.24
BC10-127	93.6	2.20	1.00	.56	.45	.68	.46	.55	.09	<.05
BC10-145	95.1	1.92	1.26	.04	<.10	<.02	.89	<.02	.08	<.05
BC10-63	57.3	14.60	10.60	.0H	2.34	.29	7.38	.11	2.25	.15
BC10-74	84.8	1.00	7.73	.0H	.21	.54	.55	<.02	.02	.13
BC11-213	95.4	2.23	.77	.05	<.10	<.02	.95	.09	.09	<.05
BC11-48	93.6	3.93	.63	.05	<.10	<.02	<.15	<.02	.15	<.05
BC16-101	53.3	14.40	11.60	.0H	4.24	1.56	5.98	.66	2.68	.40
BC16-46	43.8	9.30	29.30	.0H	.13	.17	5.22	.10	1.62	1.45
BC2-135	73.7	3.02	9.00	.0H	1.30	3.69	1.69	<.02	.33	.39
BC2-147	71.0	2.45	8.71	.0H	1.85	5.20	1.39	<.02	.36	<.05
BC2-169	49.8	17.60	10.60	8.21	6.50	1.03	4.31	1.79	1.01	.10
BC2-212	90.9	3.63	1.76	1.09	.97	.09	.92	.56	.15	.05
BC2-322	48.7	10.60	24.20	.0H	.17	.06	4.42	.04	.51	.21
BC24-120	36.6	9.11	9.24	.0H	9.37	12.40	2.44	.97	1.30	.08
BC24-82	55.8	15.10	6.83	.0H	3.01	3.12	7.40	.65	.73	.24
BC24-94	40.4	11.00	9.22	.0H	5.17	10.20	5.89	.31	.58	<.05
BC27-182	43.4	12.00	7.21	.0H	3.91	10.30	6.75	.13	.94	.15
BC27-204	43.5	14.20	12.00	8.26	6.06	7.52	4.91	1.11	2.13	.24
BC29-168	44.6	13.30	9.42	.0H	4.87	7.10	6.64	.47	.97	.21
BC29-171	45.0	12.90	8.55	.0H	3.61	7.31	7.43	.10	.81	.48
BC31-433	44.9	13.50	10.00	6.99	9.74	9.99	3.28	.43	1.10	.10
BC31-436	44.2	11.90	8.82	.0H	3.85	11.70	5.29	.31	.85	.11
BC31-476	42.5	13.50	7.64	5.61	5.67	9.14	5.60	.94	.86	.08
BC31-485	55.4	12.60	5.96	.0H	2.71	5.44	6.66	.34	.63	.27
BC31-498	52.1	16.20	6.50	.0H	2.44	5.05	7.34	.95	.77	.39
BC32-339	44.7	10.60	9.32	.0H	5.41	8.63	5.58	.07	1.05	<.05
BC32-356	46.4	11.70	9.91	.0H	5.08	7.87	5.63	.10	1.12	.06
BC32-373	42.6	13.40	11.70	7.81	6.90	9.63	4.52	.29	1.89	.21
BC32-393	44.5	14.10	11.20	.0H	7.09	9.09	4.51	.77	1.36	.12
BC32-672	91.8	2.77	1.30	.63	.72	.43	1.16	.11	.11	<.05
BC32-705	72.6	3.66	9.70	.0H	1.61	2.14	1.91	.06	.40	<.05
BC32-718	70.5	3.96	9.32	.0H	1.70	2.23	2.11	<.02	.52	<.05
BC32-742	66.8	6.99	11.00	3.54	2.79	2.13	4.37	.32	.94	.27
BC32-765	67.0	4.90	11.80	.0H	1.48	2.61	2.71	.04	.48	.18
BC32-776	45.3	15.30	10.60	6.00	7.45	11.60	3.29	.11	1.58	.17
BC34-777	42.9	12.10	7.12	.0H	5.13	9.35	6.60	.16	.77	<.05
BC34-794	45.4	16.20	11.30	5.44	5.20	11.30	4.09	.24	1.47	.14
BC34-796	39.5	10.60	9.33	.0H	3.80	15.00	4.93	.22	1.02	.13
BC34-800	44.0	12.10	9.38	.0H	3.14	10.60	6.07	.24	1.09	.08
BC34-802	43.2	13.80	10.50	6.59	4.77	10.30	5.21	1.36	1.30	.14
BC4-103	95.4	2.44	.51	.06	.11	<.02	.89	.12	.10	<.05
BC4-605	47.7	14.70	10.90	6.05	6.65	10.70	3.97	.10	1.56	.15
BC4-630	58.3	10.30	6.64	.0H	1.98	6.09	5.48	.26	.94	.45

Sample	MnO%	H_2O+%	H_2O-%	CO_2%	S_{total}%	LOI 900 °C	Al %-S	Fe %-S	Mg %-S	Ca %-S	Na %-S
BC10-101	0.15	3.90	0.13	0.01	0.40	3.18	8.90	8.50	2.70	2.800	3.60
BC10-111	1.37	.23	.05	9.85	9.32	6.80	1.10	8.90	1.80	5.300	.79
BC10-127	.14	.46	.02	.97	.07	.74	1.40	.87	.30	.630	.37
BC10-145	<.02	.47	.10	.02	.07	.59	1.10	.95	.01	.020	.72
BC10-63	<.02	1.56	.10	.04	5.98	4.81	7.90	7.10	1.30	.240	5.20
BC10-74	.63	.11	.03	.81	5.87	4.10	.51	5.40	.11	.420	.39
BC11-213	<.02	.42	.05	<.01	.20	.56	1.20	.57	.02	.007	.71
BC11-48	<.02	1.85	.09	<.01	<.01	1.73	2.20	.47	.02	.010	.03
BC16-101	.44	3.16	.31	.19	2.11	3.75	7.60	7.50	2.30	1.100	4.30
BC16-46	.65	6.00	1.71	<.01	.64	8.79	4.90	20.00	.06	.130	3.80
BC2-135	.82	.35	<.01	4.96	1.88	3.11	1.20	4.80	.61	2.100	.99
BC2-147	.97	.26	.04	7.77	1.58	5.42	1.30	6.10	1.10	3.800	1.10
BC2-169	1.55	4.67	.19	1.46	.07	5.34	9.40	7.00	3.60	.730	3.20
BC2-212	.09	.63	.02	.04	.22	.80	1.90	1.30	.56	.070	.64
BC2-322	.62	2.95	.65	.03	11.80	11.00	5.60	17.00	.06	.050	3.10
BC24-120	.26	2.87	.13	16.00	.98	16.20	5.60	7.00	5.70	9.300	2.10
BC24-82	.18	1.33	.23	4.01	1.73	4.20	8.40	4.90	1.80	2.300	5.50
BC24-94	.84	.72	.20	15.30	1.77	13.10	6.40	6.70	3.10	7.300	4.70
BC27-182	.16	.54	.19	12.50	2.69	7.17	7.00	5.30	2.40	7.600	5.30
BC27-204	.17	2.96	.14	6.37	<.01	7.56	8.30	8.80	3.70	5.600	4.00
BC29-168	.17	1.17	.17	9.76	2.63	7.46	7.60	6.80	2.90	5.100	5.10
BC29-171	.13	.11	.09	10.10	5.40	4.44	7.30	6.10	2.10	5.300	5.50
BC31-433	.21	4.03	.18	3.61	.05	5.20	7.70	7.30	5.90	7.300	2.80
BC31-436	.15	1.96	.14	8.54	4.37	5.58	6.80	6.30	2.30	8.400	4.10
BC31-476	.14	1.64	.12	12.60	.55	12.10	7.80	5.60	3.40	6.700	4.50
BC31-485	.12	.41	.05	7.10	2.63	4.11	7.10	4.20	1.60	3.900	5.00
BC31-498	.15	1.14	.04	5.80	1.47	4.58	9.00	4.60	1.40	3.600	5.50
BC32-339	.20	1.08	.13	9.66	5.82	4.78	5.10	5.60	2.70	5.300	3.60
BC32-356	.22	1.97	.19	6.73	5.17	3.89	6.70	7.00	3.00	5.700	4.30
BC32-373	.17	3.90	.09	5.59	.45	7.43	7.90	8.50	4.10	7.100	3.80
BC32-393	.16	3.35	.07	4.15	.70	5.29	8.20	8.20	4.30	6.800	3.80
BC32-672	.11	.46	<.01	.53	.30	.84	1.50	1.00	.43	.340	.89
BC32-705	1.33	.69	.05	3.25	4.63	4.63	2.00	7.00	.94	1.600	1.40
BC32-718	1.56	.33	.06	4.05	6.87	5.47	2.20	6.80	1.00	1.700	1.60
BC32-742	1.85	1.02	.03	1.86	.14	2.00	4.00	8.20	1.70	1.600	3.50
BC32-765	.98	.45	<.01	2.96	8.61	6.05	2.70	8.80	.90	2.000	2.10
BC32-776	.22	3.31	.02	1.82	.05	3.01	9.00	7.70	4.40	8.500	2.70
BC34-777	.14	.46	.04	12.30	4.94	6.87	6.90	5.00	3.00	6.800	5.10
BC34-794	.17	2.66	.03	2.19	.16	2.89	11.00	9.40	3.60	9.400	3.80
BC34-796	.21	1.72	.04	11.10	4.14	7.75	6.20	6.70	2.30	11.000	3.90
BC34-800	.16	1.54	.08	8.04	5.20	4.91	6.90	6.60	1.90	7.600	4.60
BC34-802	.19	2.80	.06	7.22	.35	9.37	8.00	7.60	2.90	7.500	4.10
BC4-103	<.02	.41	.04	<.01	.02	.56	1.20	.38	.04	.010	.64
BC4-605	.19	2.85	<.01	1.58	<.01	2.94	8.30	7.40	3.90	7.500	3.10
BC4-630	.32	.67	.12	5.81	4.28	3.56	5.50	4.70	1.10	4.100	3.90

Sample	K%-S	Ti%-S	P %-S	Ag ppm-S	As ppm-S	Au ppm	Ba ppm-S	Ce ppm-S	Co ppm-S	Cr ppm-S
BC10-101	0.52	1.10	0.130	<2	50	0.1	170	23	57	280
BC10-111	.12	.08	.100	<2	940	3.1	48	32	41	83
BC10-127	.52	.05	.020	<2	<10	<.1	790	17	7	13
BC10-145	<.05	.02	<.005	<2	170	.3	15	10	1	11
BC10-63	.11	.32	.060	<2	880	2.4	91	22	45	190
BC10-74	<.05	.01	.050	<2	870	.8	15	17	18	10
BC11-213	.08	.04	.008	<2	90	.8	290	14	5	11
BC11-48	<.05	.06	<.005	<2	30	.2	20	19	1	21
BC16-101	.57	1.00	.160	<2	100	.1	230	30	40	220
BC16-46	.09	.25	.620	8	1,500	70.0	120	65	21	110
BC2-135	<.05	.13	.130	<2	370	.3	17	9	16	7
BC2-147	<.05	.16	.010	<2	30	.2	11	13	20	17
BC2-169	1.60	.57	.040	<2	20	<.1	1,900	8	47	360
BC2-212	.44	.08	.020	<2	10	<.1	1,200	14	9	17
BC2-322	<.05	.09	.080	2	2,700	13.0	17	62	57	46
BC24-120	.93	.16	.030	<2	50	.5	150	10	44	480
BC24-82	.57	.22	.100	<2	60	<.1	130	59	24	160
BC24-94	.30	.12	<.005	<2	130	.3	380	39	48	150
BC27-182	.13	.16	.060	<2	340	.8	86	9	28	120
BC27-2041	.00	.42	.090	<2	<10	<.1	240	17	51	200
BC29-168	.43	.46	.080	<2	250	4.9	110	24	31	30
BC29-171	.10	.20	.210	<2	660	4.1	170	20	29	19
BC31-433	.40	.68	.040	<2	<10	<.1	99	6	58	680
BC31-436	.28	.26	.040	<2	820	2.8	70	4	32	230
BC31-476	.88	.38	.030	<2	160	3.9	500	20	28	97
BC31-485	.30	.30	.110	<2	340	3.3	170	26	16	45
BC31-498	.84	.30	.160	<2	.2	210	41	16	8	
BC32-339	.06	.11	.010	<2	1,100	1.4	16	<4	39	160
BC32-356	.10	.18	.020	<2	780	.9	15	<4	41	230
BC32-373	.28	.96	.050	<2	40	<.1	150	16	49	210
BC32-393	.74	.85	.050	<2	60	<.1	72	7	57	340
BC32-672	.10	.06	.020	<2	50	<.1	380	13	5	10
BC32-705	.05	.19	<.005	<2	700	2.3	74	23	22	28
BC32-718	<.05	.12	<.005	<2	1,400	2.7	22	21	23	19
BC32-742	.27	.59	.100	<2	40	<.1	270	18	33	63
BC32-765	<.05	.14	.070	<2	1,000	1.6	27	23	25	27
BC32-776	.12	1.00	.070	<2	<10	<.1	30	10	48	240
BC34-777	.16	.08	.020	<2	1,100	.4	39	8	31	23
BC34-794	.27	.48	.060	<2	20	<.1	860	10	60	400
BC34-796	.21	.30	.050	<2	830	1.1	190	6	42	200
BC34-800	.22	.20	.030	<2	860	1.4	180	6	40	160
BC34-8021	.20	.47	.060	<2	100	<.1	450	7	48	200
BC4-103	.11	.04	<.005	<2	110	.1	510	15	<1	12
BC4-605	.11	.89	.060	<2	<10	<.1	13	10	46	330
BC4-630	.22	.10	.180	<2	740	.7	24	<4	36	180

Table 4. Analytical results for rock samples from the Big Canyon area—Continued

Sample	Cu ppm-S	Eu ppm-S	Ga ppm-S	Hg ppm	La ppm-S	Li ppm-S	Mn ppm-S	Mo ppm-S	Nd ppm-S	Ni ppm-S
BC10-101	35	2	22	0.03	11	33	1,000	<2	20	190
BC10-111	43	<2	10	1.60	41	<2	9,000	<2	41	160
BC10-127	14	<2	5	.10	9	4	1,200	<2	10	22
BC10-145	20	<2	7	.57	6	<2	67	43	6	5
BC10-63	160	<2	33	.50	7	8	180	10	17	140
BC10-74	23	<2	5	.79	30	<2	4,400	<2	26	68
BC11-213	30	<2	5	.03	8	2	58	<2	8	10
BC11-48	20	<2	7	.03	9	<2	23	<2	10	6
BC16-101	140	2	17	.07	13	17	2,900	6	21	130
BC16-46	110	3	24	.58	80	<2	4,500	6	75	80
BC2-135	80	<2	7	.30	13	<2	4,400	<2	14	42
BC2-147	58	<2	9	.13	15	<2	6,800	<2	16	50
BC2-169	70	<2	23	.02	4	57	10,000	<2	7	140
BC2-212	55	<2	6	<.02	7	13	720	<2	5	27
BC2-322	630	<2	37	1.00	67	3	4,300	160	53	200
BC24-120	110	<2	15	.20	3	31	2,100	<2	8	300
BC24-82	100	<2	17	.60	33	7	1,400	3	30	93
BC24-94	280	<2	20	.69	23	2	6,000	<2	26	180
BC27-182	13	<2	21	.13	3	3	1,300	<2	10	93
BC27-204	33	<2	23	.06	5	25	1,300	<2	13	160
BC29-168	110	<2	20	.89	11	10	1,300	<2	15	36
BC29-171	28	<2	23	.91	9	<2	990	<2	14	41
BC31-433	66	<2	15	.03	<2	39	1,700	<2	7	390
BC31-436	42	<2	14	.78	<2	19	1,200	<2	4	110
BC31-476	120	<2	20	.64	10	11	1,100	<2	13	50
BC31-485	120	<2	20	.55	12	3	900	<2	16	20
BC31-498	12	<2	21	.07	20	9	1,100	<2	23	14
BC32-339	62	<2	15	.36	<2	7	1,300	<2	5	170
BC32-356	12	<2	30	.16	<2	15	1,600	22	<4	190
BC32-373	57	<2	22	.03	6	36	1,300	<2	14	150
BC32-393	83	<2	20	.07	<2	34	1,300	<2	8	230
BC32-672	63	<2	5	.12	8	3	880	3	8	16
BC32-705	130	<2	15	.43	30	4	9,400	<2	31	45
BC32-718	170	<2	16	.61	27	3	11,000	<2	27	41
BC32-742	83	<2	23	.03	17	14	13,000	<2	18	70
BC32-765	24	<2	17	.42	30	3	7,100	<2	27	100
BC32-776	85	<2	22	.02	3	20	1,800	<2	10	150
BC34-777	44	<2	17	.32	3	4	1,100	<2	7	37
BC34-794	76	<2	25	.04	<2	30	1,500	<2	10	200
BC34-796	53	<2	15	.29	<2	13	1,600	4	7	89
BC34-800	65	<2	17	.36	2	13	1,200	2	5	87
BC34-802	87	<2	19	.08	<2	25	1,500	<2	7	94
BC4-103	18	<2	4	.05	9	3	30	<2	7	4
BC4-605	82	<2	20	<.02	3	20	1,400	<2	11	150
BC4-630	89	<2	22	.86	<2	5	2,100	690	5	140

Sample	Pb ppm-S	Sb ppm-S	Sc ppm-S	Se ppm	Sr ppm-S	Te ppm	V ppm-S	Y ppm-S	Yb ppm-S	Zn ppm-S	Type
BC10-101	<4	0.6	44	<0.1	69	0.130	330	36	4	170	25
BC10-111	8	6.2	13	2.3	210	1.200	83	14	1	190	24
BC10-127	<4	.6	4	<.1	16	.050	27	3	<1	23	13
BC10-145	4	11.0	3	.4	3	.100	25	<2	<1	6	12
BC10-63	<4	3.3	32	1.6	23	.450	150	7	<1	89	24
BC10-74	5	4.2	3	1.2	19	.430	40	8	<1	120	12
BC11-213	<4	.6	3	<.2	4	.060	15	2	<1	11	12
BC11-48	<4	.6	7	<.1	<2	.120	40	5	<1	9	12
BC16-101	<4	1.1	34	.5	39	.130	220	30	3	110	25
BC16-46	20	6.7	22	<2.0	120	.830	84	17	2	110	24
BC2-135	7	2.2	6	<2.0	82	.300	230	7	<1	44	15
BC2-147	7	1.4	10	.6	140	.260	360	5	<1	52	15
BC2-169	11	.7	36	.4	29	.044	220	28	3	92	25
BC2-212	7	.5	6	<.1	30	.150	20	4	<1	41	12
BC2-322	23	9.4	22	18.0	28	2.200	78	14	3	120	24
BC24-120	<4	1.7	28	.6	410	.062	270	14	2	80	24
BC24-82	13	2.5	15	4.4	130	.210	110	17	2	110	25
BC24-94	15	3.4	16	6.9	470	.890	94	13	2	72	25
BC27-182	<4	1.1	18	1.9	350	.078	230	12	1	55	24
BC27-204	<4	.8	37	<2.0	190	<.020	310	21	3	97	25
BC29-168	<4	2.2	26	1.3	500	.082	480	15	2	62	24
BC29-171	<4	4.0	16	3.2	400	.290	49	18	1	45	24
BC31-433	<4	.1	35	<5.0	130	<.020	210	22	3	70	25
BC31-436	4	3.4	31	2.1	300	.130	180	12	2	28	24
BC31-476	<4	1.1	21	<1.0	390	.087	390	10	1	69	25
BC31-485	<4	1.7	11	1.1	220	.190	110	13	1	52	24
BC31-498	<4	.6	9	.4	370	.023	130	16	2	54	24
BC32-339	<4	2.6	22	<2.0	290	.410	200	9	1	60	24
BC32-356	<4	1.6	30	<2.0	280	.580	370	14	2	49	24
BC32-373	<4	.5	34	<.5	220	.042	280	29	3	86	25
BC32-393	<4	.6	39	<.2	150	.045	260	30	3	92	25
BC32-672	6	.4	4	<.1	29	.300	94	3	<1	34	15
BC32-705	14	2.7	9	<2.0	74	.550	130	7	<1	96	14
BC32-718	17	3.4	10	<5.0	110	1.000	41	6	<1	120	14
BC32-742	12	.9	17	<.2	49	.065	330	14	2	150	14
BC32-765	7	3.1	8	11.0	100	.770	96	10	1	140	14
BC32-776	<4	.4	37	.5	200	<.020	280	30	3	66	25
BC34-777	<4	2.6	26	<2.0	400	.170	63	7	<1	29	24
BC34-794	<4	.6	50	<.2	200	<.020	310	36	4	120	25
BC34-796	<4	2.3	43	<2.0	680	1.200	430	19	2	69	24
BC34-800	<4	2.3	38	<2.0	520	.440	340	12	1	64	24
BC34-802	<4	.8	44	<.2	240	.060	310	10	2	92	25
BC4-103	<4	.4	4	<.5	8	.048	26	<2	<1	<4	12
BC4-605	<4	.3	40	<2.0	150	<.020	260	30	4	92	25
BC4-630	37	1.0	20	4.0	83	2.400	140	14	1	53	25

Sample	SiO_2%	Al_2O_3%	$FeTO_3$%	FeO%	MgO%	CaO%	Na_2O%	K_2O%	TiO_2%	P_2O_5%
BC4-656	45.0	5.69	11.10	0.0H	2.25	10.50	2.25	0.79	1.94	0.16
BC4-669	44.9	12.10	5.79	.0H	2.67	12.70	6.04	.44	.58	<.05
BC4-683	39.6	11.10	8.19	.0H	5.38	12.60	4.80	.54	1.04	<.05
BC4-701	41.5	11.00	8.79	.0H	5.82	9.90	5.73	.16	.98	<.05
BC4-773	43.7	12.00	6.93	.0H	4.87	8.85	6.91	.09	.76	.18
BC4-781	42.4	14.10	8.22	6.01	7.36	7.85	5.28	.68	.93	.09
BC4-88	94.0	.79	3.57	.06	<.10	<.02	.33	<.02	.08	<.05
BC4-92	92.0	.69	4.60	.09	<.10	<.02	.28	<.02	.05	<.05
BC5-95	65.8	14.20	6.63	.0H	.85	.17	4.78	.04	1.47	.11
BC5-98	83.1	1.81	8.37	.0H	.96	.53	1.57	<.02	.10	.10
BC7-25	73.2	8.34	9.99	.29	.17	.05	4.57	.10	1.29	.08
BC7-55	.0H	.0H	.0H	.0H	.0H	.0H	.0H	.0H	.0H	.0H
BC8-135	94.3	2.18	.95	.52	.47	.03	.51	.22	.08	<.05
BC8-218	46.2	19.30	21.40	<.01	.11	<.02	.23	<.02	.80	.28
BC8-252	73.1	2.65	18.70	.04	<.10	<.02	.23	<.02	.52	.61
BC8-499	49.0	12.50	8.62	.0H	4.67	8.14	6.32	.55	.94	.07
BC8-501	48.0	14.40	11.80	.0H	7.00	4.33	5.14	2.21	1.16	.08
BC8-84	88.3	5.67	1.65	.06	.19	.04	1.34	.50	.23	<.05
BC9-185	94.3	2.18	1.21	.86	.62	.07	.61	.17	.09	<.05
BC9-210	94.5	1.91	1.38	.72	.55	.07	.47	.27	.08	<.05
BC9-225	51.3	20.10	6.96	5.02	7.05	.20	2.90	3.43	.96	<.05
BC9-243	79.2	4.53	9.33	.0H	.18	.04	1.71	<.02	.53	<.05
BC9-348	46.1	14.40	11.20	7.74	10.60	10.10	2.59	.12	1.07	.07
LO4-116	43.3	15.60	10.50	7.67	6.71	8.93	4.72	.73	1.16	.11
LO4-124	41.5	12.70	8.49	.0H	4.40	11.30	5.59	.99	.82	.14
LO4-146	37.9	10.90	9.03	.0H	6.12	11.50	5.18	1.01	1.27	.21
LO4-157	40.8	13.60	10.30	7.84	6.82	10.20	4.49	.74	1.48	.16
LO5-125	41.7	15.60	11.50	7.86	8.89	8.27	3.27	1.72	1.12	.12
LO5-42	33.7	9.30	8.04	.0H	7.62	14.30	5.06	.18	.48	.12
LO5-46	43.5	12.10	7.70	.0H	4.04	9.01	6.38	.86	1.73	.35
LO7-102	49.0	14.00	5.37	.0H	3.49	7.13	7.96	.12	1.14	.10
LO7-109	43.8	12.30	5.74	.0H	4.80	9.95	6.67	.42	.95	.11
LO7-125	46.8	12.40	9.76	6.07	5.38	6.46	6.28	.73	2.07	.27
LO7-142	42.7	12.20	6.25	.0H	5.02	10.20	6.81	.30	.67	<.05
LO7-59	38.7	11.10	10.30	.0H	6.87	9.87	5.22	.40	1.22	.08
LO7-75	46.1	14.70	11.80	7.81	6.83	6.39	5.13	.56	1.96	.23
LO7-86	44.9	13.60	10.10	.0H	5.57	5.69	5.84	1.12	1.66	.15

Sample	MnO%	H_2O^+%	H_2O^-%	CO_2%	S_{total}%	LOI 900 °C	Al %-S	Fe %-S	Mg %-S	Ca %-S	Na %-S
BC4-656	0.23	1.00	0.06	10.00	9.67	4.57	3.10	7.30	1.30	7.700	1.60
BC4-669	.25	1.22	.20	10.70	3.51	6.95	6.70	3.80	1.50	9.200	4.50
BC4-683	.26	1.69	<.01	13.30	3.48	10.10	6.30	5.50	3.10	9.200	3.70
BC4-701	.18	1.11	.03	13.10	3.18	9.01	6.30	5.90	3.40	7.300	4.40
BC4-773	.19	.31	.04	12.60	4.38	6.52	6.70	4.50	2.80	6.400	5.00
BC4-781	.18	2.87	.06	10.50	.35	11.60	8.00	5.50	4.20	5.800	4.00
BC4-88	<.02	.88	.06	.03	.13	1.11	.37	2.70	.01	.009	.19
BC4-92	.04	1.00	.04	.02	.28	1.35	.32	3.50	.02	.020	.15
BC5-95	.03	3.79	.71	.02	.84	4.65	7.40	4.30	.46	.140	3.30
BC5-98	.60	.49	.04	.94	1.79	1.69	.91	6.00	.57	.430	1.20
BC7-25	.04	1.96	.12	.02	.02	2.21	4.50	7.10	.08	.050	3.40
BC7-55	.0H	1.22	.41	1.64	17.70	.0H	3.00	24.00	.78	.530	2.50
BC8-135	.10	.56	.10	<.01	.03	.84	1.10	.65	.26	.030	.30
BC8-218	.10	10.00	1.88	<.01	.02	11.40	10.00	14.00	.04	.030	.02
BC8-252	<.02	3.74	.67	<.01	.02	4.11	1.40	13.00	.01	.010	.01
BC8-499	.12	1.60	.20	4.77	4.00	3.10	6.80	5.50	2.60	5.900	4.50
BC8-501	.15	2.77	.11	1.92	2.36	2.86	7.80	7.60	3.80	3.200	3.70
BC8-84	<.02	1.38	.10	<.01	<.01	1.55	3.10	1.20	.09	.040	.97
BC9-185	.23	.51	.04	<.01	.05	.41	1.10	.90	.35	.070	.39
BC9-210	.24	.54	.04	.01	.11	.54	1.00	1.00	.33	.060	.27
BC9-225	.43	5.85	.48	<.01	.09	5.49	11.00	4.70	3.90	.160	2.10
BC9-243	.14	1.14	.22	.02	4.56	3.98	2.50	6.60	.09	.040	1.30
BC9-348	.17	4.01	.05	.78	.03	2.90	8.20	7.50	5.90	7.500	2.00
L04-116	.15	4.07	.08	5.51	.02	8.32	8.70	7.10	3.80	6.200	3.60
L04-124	.16	1.50	.07	10.60	3.12	8.37	7.00	5.70	2.50	7.500	4.20
L04-146	.20	.94	.05	14.10	3.16	10.10	6.10	6.10	3.50	8.100	4.00
L04-157	.23	3.83	.09	8.52	.02	11.10	7.70	6.90	3.90	7.200	3.50
L05-125	.16	4.54	.06	4.20	<.01	7.98	8.90	7.50	4.70	5.700	2.80
L05-42	.28	.96	.06	19.80	1.52	17.70	5.30	5.50	4.50	10.000	4.00
L05-46	.16	.53	.04	11.40	3.65	6.85	6.70	5.10	2.30	6.100	4.70
L07-102	.11	.22	<.01	10.40	2.10	6.97	7.50	3.50	2.00	5.000	5.60
L07-109	.15	.48	.01	14.10	1.36	11.50	6.90	3.90	2.80	7.000	5.10
L07-125	.12	1.80	.08	2.25	.01	9.14	7.10	6.70	3.20	4.600	4.90
L07-142	.15	.29	<.01	15.40	1.36	12.40	6.80	4.20	3.00	7.300	5.10
L07-59	.16	1.44	.02	12.90	3.10	9.72	6.40	7.00	4.00	6.900	4.20
L07-75	.19	3.53	.07	3.48	.56	5.41	8.20	7.90	3.90	4.500	4.00
L07-86	.12	1.86	.02	7.76	3.09	5.80	7.50	6.80	3.10	4.000	4.30

Table 4. Analytical results for rock samples from the Big Canyon area—Continued

Sample	K %-S	Ti %-S	P %-S	Ag ppm-S	As ppm-S	Au ppm	Ba ppm-S	Ce ppm-S	Co ppm-S	Cr ppm-S
BC4-656	0.67	0.06	0.050	34	700	2.1	20	<4	100	140
BC4-669	.40	.09	.009	3	440	.9	20	12	29	150
BC4-683	.51	.17	<.005	<2	270	4.2	13	5	38	310
BC4-701	.16	.17	.006	<2	260	4.8	11	5	39	250
BC4-773	.09	.07	.070	<2	670	.7	14	8	29	120
BC4-781	.63	.20	.030	<2	10	.1	87	10	37	58
BC4-88	<.05	.03	<.005	<2	610	.5	28	10	2	19
BC4-92	<.05	.02	.009	<2	480	.4	13	8	3	11
BC5-95	<.05	.29	.040	15	160	.6	8	5	6	250
BC5-98	<.05	.06	.040	<2	300	.9	20	19	23	4
BC7-25	.10	.27	.030	<2	600	1.8	13	24	2	49
BC7-55	.09	.16	.190	<2	3,200	9.0	11	91	75	32
BC8-135	.17	.05	<.005	<2	<10	<.1	710	15	5	10
BC8-218	<.05	.17	.130	<2	730	8.0	89	96	13	210
BC8-252	<.05	.19	.260	<2	550	1.7	21	18	3	79
BC8-499	.50	.46	.030	<2	870	1.1	12	<4	39	360
BC8-501	1.90	.66	.030	<2	550	.1	140	6	55	520
BC8-84	.42	.14	<.005	<2	30	<.1	1,000	21	2	28
BC9-185	.15	.06	.009	<2	10	<.1	680	14	12	12
BC9-210	.21	.05	.020	<2	<10	<.1	320	16	13	10
BC9-225	3.00	.56	.020	<2	<10	<.1	6,200	25	40	390
BC9-243	<.05	.33	.010	<2	530	1.1	35	17	14	34
BC9-348	.12	.63	.030	<2	<10	<.1	18	4	58	590
LO4-116	.67	.48	.040	<2	<10	<.1	270	5	56	470
LO4-124	.88	.18	.060	<2	490	1.1	320	<4	47	610
LO4-146	.92	.34	.090	<2	720	1.6	230	7	43	330
LO4-157	.68	.35	.060	<2	20	<.1	42	7	50	370
LO5-125	1.60	.43	.050	<2	20	<.1	470	5	60	800
LO5-42	.17	.04	.050	<2	200	.4	150	7	26	140
LO5-46	.78	.21	.160	<2	560	1.7	140	16	27	130
LO7-102	.11	.23	.040	<2	220	.4	23	5	25	300
LO7-109	.40	.20	.040	<2	170	.5	100	5	24	330
LO7-125	.68	.53	.110	<2	<10	<.1	310	15	44	330
LO7-142	.27	.12	<.005	<2	140	.2	38	<4	24	130
LO7-59	.36	.19	.040	<2	210	1.7	52	<4	54	400
LO7-75	.53	.62	.100	<2	<10	<.1	130	11	52	340
LO7-86	.98	.40	.060	<2	320	1.2	200	10	40	280

Sample	Cu ppm-S	Eu ppm-S	Ga ppm-S	Hg ppm	La ppm-S	Li ppm-S	Mn ppm-S	Mo ppm-S	Nd ppm-S	Ni ppm-S
BC4-656	47	<2	37	6.30	<2	7	1,700	14,000	<4	290
BC4-669	18	<2	28	.77	4	8	1,800	1,100	8	110
BC4-683	33	<2	24	.36	<2	15	1,900	31	<4	190
BC4-701	20	<2	23	.20	<2	10	1,300	32	<4	200
BC4-773	39	<2	20	.25	<2	<2	1,300	9	7	130
BC4-781	97	<2	18	.20	<2	27	1,300	2	6	53
BC4-88	89	<2	7	.20	9	<2	190	2	7	4
BC4-92	84	<2	4	.49	8	<2	380	<2	7	5
BC5-95	37	<2	34	.74	2	5	270	1,700	5	44
BC5-98	300	<2	8	.30	24	7	4,500	10	20	89
BC7-25	40	<2	17	.32	17	2	400	<2	21	16
BC7-55	1,000	3	27	1.20	140	10	11,000	22	92	250
BC8-135	18	<2	4	.03	8	5	720	<2	8	22
BC8-218	480	6	24	.30	140	5	750	480	150	73
BC8-252	200	<2	10	.38	20	<2	220	61	23	9
BC8-499	40	<2	14	.09	<2	14	890	17	<4	220
BC8-501	83	<2	18	.03	<2	35	1,000	<2	6	290
BC8-84	44	<2	7	.12	10	5	86	8	8	5
BC9-185	33	<2	5	<.02	9	8	1,700	<2	9	31
BC9-210	42	<2	4	.05	11	7	1,700	<2	11	67
BC9-225	100	<2	17	.03	13	59	3,000	2	19	200
BC9-243	320	<2	7	.18	19	<2	1,100	9	18	67
BC9-348	100	<2	17	<.02	<2	21	1,300	<2	6	360
LO4-116	37	<2	17	.02	<2	44	1,100	<2	5	250
LO4-124	130	<2	16	.13	<2	16	1,200	<2	<4	240
LO4-146	39	<2	17	.05	<2	10	1,500	<2	5	180
LO4-157	50	<2	17	.02	2	37	1,700	<2	6	210
LO5-125	110	<2	18	<.02	<2	52	1,200	<2	5	350
LO5-42	5	<2	17	.03	<2	3	2,100	<2	5	150
LO5-46	20	<2	17	.08	6	<2	1,100	<2	13	110
LO7-102	8	<2	19	.06	<2	<2	800	<2	<4	110
LO7-109	9	<2	17	.09	<2	2	1,100	<2	4	130
LO7-125	81	<2	15	.02	6	13	940	<2	15	220
LO7-142	10	<2	17	.03	<2	<2	1,100	<2	<4	90
LO7-59	77	<2	13	.09	<2	12	1,200	<2	<4	270
LO7-75	76	<2	21	.08	4	29	1,400	<2	11	210
LO7-86	100	<2	16	.08	3	14	870	<2	7	130

Table 4. Analytical results for rock samples from the Big Canyon area—Continued

Sample	Pb ppm-S	Sb ppm-S	Sc ppm-S	Se ppm	Sr ppm-S	Te ppm	V ppm-S	Y ppm-S	Yb ppm-S	Zn ppm-S	Type
BC4-656	570	69.0	28	10.0	70	22.000	220	9	1	35	24
BC4-669	15	4.3	22	2.6	90	1.000	120	9	<1	30	25
BC4-683	<4	2.0	33	1.0	170	.280	230	11	2	53	24
BC4-701	<4	1.3	31	.6	390	.230	380	8	1	49	24
BC4-773	<4	1.8	20	1.5	310	.290	70	11	1	24	25
BC4-781	<4	2.6	33	.4	230	<.020	230	8	<1	79	25
BC4-88	<4	2.4	2	<2.0	<2	.470	95	<2	<1	8	12
BC4-92	<4	.9	2	2.5	<2	.440	93	<2	<1	8	12
BC5-95	10	1.7	36	2.0	10	1.200	370	9	1	23	25
BC5-98	6	2.0	5	.4	56	.420	65	8	1	100	12
BC7-25	<4	3.6	10	1.1	11	.300	300	4	<1	41	24
BC7-55	11	9.4	15	<5.0	21	2.000	870	29	4	340	11
BC8-135	<4	.2	4	<.1	14	.130	26	8	<1	27	13
BC8-218	43	5.1	65	4.6	7	2.600	270	59	8	91	11
BC8-252	20	5.3	19	5.8	9	1.000	160	6	<1	26	11
BC8-499	<4	2.8	28	1.1	84	.090	160	14	2	49	24
BC8-501	<4	1.9	39	.5	52	.020	200	21	3	90	25
BC8-84	8	.9	8	.3	48	.150	43	3	<1	17	15
BC9-185	<4	.3	3	<.1	19	.068	17	9	<1	34	12
BC9-210	<4	.5	3	<.1	6	.110	10	7	<1	38	12
BC9-225	<4	1.4	37	.1	140	<.020	220	50	3	120	25
BC9-243	32	3.8	12	1.4	16	.240	17	15	1	71	15
BC9-348	<4	.2	37	.2	130	<.020	220	24	3	75	25
L04-116	5	.4	36	<.5	99	<.020	210	24	3	88	25
L04-124	<4	3.0	28	2.4	410	.038	310	12	1	92	24
L04-146	<4	2.6	34	3.0	410	.029	270	15	2	59	24
L04-157	<4	.9	35	<.2	190	<.020	230	11	2	86	25
L05-125	<4	.6	36	<.2	160	<.020	200	23	3	97	25
L05-42	<4	1.3	11	1.4	530	.063	80	13	2	83	25
L05-46	<4	43.0	11	3.1	330	.056	96	17	2	46	24
L07-102	<4	1.0	12	1.2	250	.048	150	7	<1	22	25
L07-109	<4	.8	20	1.4	340	.029	230	9	1	31	25
L07-125	<4	1.6	47	<.2	210	<.020	490	16	3	90	26
L07-142	<4	.6	17	3.5	360	.038	79	6	<1	26	25
L07-59	5	1.1	30	1.6	350	.062	290	8	1	66	24
L07-75	<4	1.1	38	.4	110	<.020	250	16	2	95	26
L07-86	<4	1.8	33	2.0	210	.032	280	9	1	68	24

[1]Results are not included for some ICP-AES determinations in which detectable amounts were present in only a few samples. Au detected in 4 samples (8-92 ppm); Be detected in 7 samples (1-3 ppm); Cd detected in one sample (3 ppm); Th detected in 10 samples (4-9 ppm); U detected in no samples with limit of detection 10 ppm.

[2]Type: Two characters describe character of sample analyzed. First character is protolith type: 1, metachert; 2, mafic igneous rock. Second character is alteration and mineralization character: 1, pyritic metachert, gold assay > 1 ppm; 2, pyritic metachert, gold assay < 1 ppm; 3, barren metachert, PCA alteration, gold assay > 1 ppm; 4, PCA alteration, gold assay < 1 ppm; 5, PCA alteration, barren; 6, barren and slightly altered mafic rock.

[3]Total iron reported as Fe_2O_3.

Table 5. Lower limits of determination in geochemical analyses

Major elements, in weight percent			
SiO_2	0.05	TiO_2	0.02
Al_2O_3	0.10	P_2O_3	0.05
[1]$FeTO_3$	0.04	MnO	0.02
FeO	0.01	H_2O^+	0.01
MgO	0.10	H_2O^-	0.01
CaO	0.05	CO_2	0.01
Na_2O	0.15	S_{total}	0.01
K_2O	0.02		
[2]Al (S)	0.05	Mg (S)	0.005
Ca (S)	0.05	Na (S)	0.005
Fe (S)	0.05	P (S)	0.005
K (S)	0.05	Ti (S)	0.005

Minor elements, in parts per million			
Ag	2	Mn	4
As	10	Mo	2
Au	0.05	Nb	4
Ba	1	Nd	4
Be	1	Ni	2
Bi	10	Pb	4
Cd	2	Sc	2
Ce	4	Se	0.01
Co	1	Sn	10
Cr	1	Sr	2
Cu	1	Ta	40
Eu	2	Te	0.05
Ga	4	Th	4
Hg	0.02	V	2
Ho	4	Y	2
La	2	Yb	1
Li	2	Zn	2

[1]Total iron reported as Fe_2O_3.

[2](S), determined by induction-coupled plasma atomic emission spectrometry.

SELECTED SERIES OF U.S. GEOLOGICAL SURVEY PUBLICATIONS

Periodicals

Earthquakes & Volcanoes (issued bimonthly).
Preliminary Determination of Epicenters (issued monthly).

Technical Books and Reports

Professional Papers are mainly comprehensive scientific reports of wide and lasting interest and importance to professional scientists and engineers. Included are reports on the results of resource studies and of topographic, hydrologic, and geologic investigations. They also include collections of related papers addressing different aspects of a single scientific topic.

Bulletins contain significant data and interpretations that are of lasting scientific interest but are generally more limited in scope or geographic coverage than Professional Papers. They include the results of resource studies and of geologic and topographic investigations; as well as collections of short papers related to a specific topic.

Water-Supply Papers are comprehensive reports that present significant interpretive results of hydrologic investigations of wide interest to professional geologists, hydrologists, and engineers. The series covers investigations in all phases of hydrology, including hydrogeology, availability of water, quality of water, and use of water.

Circulars present administrative information or important scientific information of wide popular interest in a format designed for distribution at no cost to the public. Information is usually of short-term interest.

Water-Resources Investigations Reports are papers of an interpretive nature made available to the public outside the formal USGS publications series. Copies are reproduced on request unlike formal USGS publications, and they are also available for public inspection at depositories indicated in USGS catalogs.

Open-File Reports include unpublished manuscript reports, maps, and other material that are made available for public consultation at depositories. They are a nonpermanent form of publication that may be cited in other publications as sources of information.

Maps

Geologic Quadrangle Maps are multicolor geologic maps on topographic bases in 7 1/2- or 15-minute quadrangle formats (scales mainly 1:24,000 or 1:62,500) showing bedrock, surficial, or engineering geology. Maps generally include brief texts; some maps include structure and columnar sections only.

Geophysical Investigations Maps are on topographic or planimetric bases at various scales; they show results of surveys using geophysical techniques, such as gravity, magnetic, seismic, or radioactivity, which reflect subsurface structures that are of economic or geologic significance. Many maps include correlations with the geology.

Miscellaneous Investigations Series Maps are on planimetric or topographic bases of regular and irregular areas at various scales; they present a wide variety of format and subject matter. The series also includes 7 1/2-minute quadrangle photogeologic maps on planimetric bases which show geology as interpreted from aerial photographs. Series also includes maps of Mars and the Moon.

Coal Investigations Maps are geologic maps on topographic or planimetric bases at various scales showing bedrock or surficial geology, stratigraphy, and structural relations in certain coal-resource areas.

Oil and Gas Investigations Charts show stratigraphic information for certain oil and gas fields and other areas having petroleum potential.

Miscellaneous Field Studies Maps are multicolor or black-and-white maps on topographic or planimetric bases on quadrangle or irregular areas at various scales. Pre-1971 maps show bedrock geology in relation to specific mining or mineral-deposit problems; post-1971 maps are primarily black-and-white maps on various subjects such as environmental studies or wilderness mineral investigations.

Hydrologic Investigations Atlases are multicolored or black-and-white maps on topographic or planimetric bases presenting a wide range of geohydrologic data of both regular and irregular areas; principal scale is 1:24,000 and regional studies are at 1:250,000 scale or smaller.

Catalogs

Permanent catalogs, as well as some others, giving comprehensive listings of U.S. Geological Survey publications are available under the conditions indicated below from the U.S. Geological Survey, Books and Open-File Reports Section, Federal Center, Box 25425, Denver, CO 80225. (See latest Price and Availability List.)

"Publications of the Geological Survey, 1879-1961" may be purchased by mail and over the counter in paperback book form and as a set of microfiche.

"Publications of the Geological Survey, 1962-1970" may be purchased by mail and over the counter in paperback book form and as a set of microfiche.

"Publications of the U.S. Geological Survey, 1971-1981" may be purchased by mail and over the counter in paperback book form (two volumes, publications listing and index) and as a set of microfiche.

Supplements for 1982, 1983, 1984, 1985, 1986, and for subsequent years since the last permanent catalog may be purchased by mail and over the counter in paperback book form.

State catalogs, "List of U.S. Geological Survey Geologic and Water-Supply Reports and Maps For (State)," may be purchased by mail and over the counter in paperback booklet form only

"Price and Availability List of U.S. Geological Survey Publications," issued annually, is available free of charge in paperback booklet form only.

Selected copies of a monthly catalog "New Publications of the U.S. Geological Survey" available free of charge by mail or may be obtained over the counter in paperback booklet form only. Those wishing a free subscription to the monthly catalog "New Publications of the U.S. Geological Survey" should write to the U.S. Geological Survey, 582 National Center, Reston, VA 22092.

Note.--Prices of Government publications listed in older catalogs, announcements, and publications may be incorrect. Therefore, the prices charged may differ from the prices in catalogs, announcements, and publications.